HELSINKI UNIVERSITY OF TECHNOLOGY
Department of Electrical and Communications Engineering

Miia Pitkonen

The evolution of diffusion tensor parameters and relaxation times after experimental ischemic stroke

Thesis submitted in partial fulfillment of the requirements for the degree of Master of Science in Engineering, 7.10.2008 Espoo

Supervisor of the Thesis: Mikko Sams

Instructors of the Thesis: Usama Abo Ramadan, Turgut Tatlisumak

TEKNILLINEN KORKEAKOULU

DIPLOMITYÖN TIIVISTELMÄ

Tekijä: Miia Pitkonen

Työn nimi: The evolution of diffusion tensor parameters and relaxation times after experimental ischemic stroke

Päivämäärä: 7.10.2008 Sivumäärä: 9+72

Osasto: Sähkö- ja tietoliikennetekniikan osasto

Professuuri: S-114

Työn valvoja: Mikko Sams

Työn ohjaaja: Usama Abo Ramadan, Turgut Tatlisumak

Teksti: Työssä seurattiin kuinka diffuusiotensoriparametrit (fractional anisotropy (FA) ja apparent diffusion coefficient (ADC)), T1- ja T2- relaksaatioajat kehittyvät aivoinfarktin jälkeisessä aivokudoksessa. Erityisesti kiinnostuksen kohteena oli anisotropiaa/isotropiaa määrittävä FA-parametri, jonka luonnetta ei ole vielä yleisesti täysin selvitetty. Mielenkiinnon kohteena olivat myös eri aivoalueiden väliset erot näitä parametreja tarkasteltaessa. Aivoinfarktia mallinnettiin Wistar-rotilla, joille se toteutettiin estämällä veren kulku oikean keskimmäisen aivovaltimon kautta aivokudokseen joko pysyvällä tai 90 minuutin ohimenevällä sululla (n = 9 eläintä/ryhmä). Ryhmät kuvattiin aikapisteissä 2 ja 3.5 tuntia, 1, 2, 3 ja 4 päivää, 1, 2, 4, 6 ja 8 viikkoa. Operoitujen eläinten lisäksi tutkimuksessa oli mukana ryhmä täysin terveitä rottia (n = 8). Magneettikuvantaminen toteutettiin 4.7 Teslan kuvauslaitteella.

Patologinen tila kuten aivoinfarkti saa aivokudoksessa aikaan järjestäytyneiden rakenteiden vaurioitumista ja jopa tuhoutumista. ADC-parametri rekisteröi muutokset, jotka ovat yhteydessä solujen vesipitoisuuteen kun taas FA-parametri kuvaa muutoksia mikrorakenteissa.

Mittaukset osoittivat, että aivoinfarktin seurauksena iskemisen kudoksen FA-arvo laskee voimakkaasti akuutissa ja akuutin jälkeisessä vaiheessa. Pysyvän sulun jälkeisessä tapauksessa harmaan aineen alueella lasku on kuitenkin voimakkaampaa kuin valkean aineen alueella. Ohimenevän sulun jälkeisessä tapauksessa valkean aineen FA-arvo laskee voimakkaammin kuin harmaan aineen alueella. Kroonisessa vaiheessa FA-arvo normalisoituu. Verrattaessa pysyvää ja ohimenevää sulkua huomattiin ADC-arvon kehityksen olevan edellä ohimenevän sulun tapauksessa kun taas muut parametrit eivät juuri eronneet näiden kahden ryhmän välillä. Myöhemmin ADC- arvot palautuvat ja nousevat normaalitasoa korkeammiksi. Työssä verrattiin myös iskemisen alueen tilavuutta, joka oli lähes poikkeuksetta aina suurempi pysyvän sulun tapauksessa.

Tulokset eri aivoalueilta osoittavat, että diffuusiotensoriparametrit tarjoavat mahdollisuuden määrittää kuvausprotokollia, jotka kuvaavat entistä tarkemmin aivoinfarktin jälkeistä kudosta.

Avainsanat: aivojen kuvantaminen, diffuusiotensorikuvantaminen, magneettinen resonanssi, MRI, aivoinfarkti

HELSINKI UNIVERSITY OF TECHNOLOGY

ABSTRACT OF THE MASTER'S THESIS

Author: Miia Pitkonen

Name of the Thesis: The evolution of diffusion tensor parameters and relaxation times after experimental ischemic stroke

Date: 7.10.2008 Number of pages: 9+72

Department: Department of Electrical and Communications Engineering

Professorship: S-114

Supervisor: Mikko Sams

Instructor: Usama Abo Ramadan, Turgut Tatlisumak

Text: The temporal evolution of the diffusion tensor imaging (DTI) parameters (fractional anisotropy (FA) and apparent diffusion coefficient (ADC)), T1- and T2 relaxation times were measured after stroke in ischemic brain tissue. FA-parameter describes anisotropy/isotropy and it was the most central parameter in this work. It was also compared whether different brain regions have characteristic behavior after ischemia.

Wistar rats were subjected to focal cerebral ischemia by suture occlusion of MCA (MCAO) for 90 minutes followed by reperfusion (n = 9), or permanent occlusion (n = 9). They were imaged 2 and 3.5 hours, 1, 2, 3, and 4 days, 1, 2, 4, 6, and 8 weeks after the MCAO. Healthy rats were used as controls (n = 8). The MRI measurements were performed with a 4.7 T MR Scanner. The temporal evolution of diffusion tensor indices (ADC and FA), T1, and T2 were measured.

A pathologic condition like brain ischemia causes structural damage to the tissue that give rise to a loss of organization and structure at the cellular level. The changes in water apparent diffusion are thought to be related to changes in brain water content while the changes in anisotropy are linked to changes in tissues microstructure.

In the acute and subacute phase after permanent MCAO, FA reduced more rapidly and under longer period of time in gray matter (GM) than in white matter (WM). After transient MCAO, FA reduced more rapidly in WM than in GM. In the chronic phase, FA normalized. While comparing between transient and permanent ischemia, reperfusion accelerated the evolution of ADC, while the other parameters showed only minor difference between these two groups. From the comparison of lesion volumes, it was concluded that permanent ischemia is causing more severe ischemia whereas early reperfusion salvage penumbra.

The observations of DTI parameters from different brain regions suggest a more comprehensive protocol for the description of ischemia.

Keywords: brain imaging, diffusion tensor imaging (DTI), magnetic resonance, MRI, stroke

Foreword

This Master's thesis has been carried out at the Experimental MRI Laboratory, at the Department of Neurology, at the Helsinki University Central Hospital. I have been very lucky to work in this research group which provided excellent circumstances and good spirit to do this work. I want to thank Docent Turgut Tatlisumak for being my supervisor and for giving me the possibility to work on this field that I so much enjoy. My sincere thanks go to my other supervisor Usama Abo-Ramadan who introduced me to the field of medical imaging. His insight and experience about imaging have guided me through this challenging project. I also want to thank for sharing numerous humorous discussions during the past years.

Special thanks go to my co-workers Aysan Durukan, Eric Pedrono, and Ivan Marincovic for carrying out the surgical procedures for this project, and for friendship.

However, my dearest thanks go to my mother, father, and my little sister.

Acknowledgement

This study was supported by a grant from Finnish Cultural Foundation.

Thank you all.

Helsinki, October 2008

Miia Pitkonen

List of symbols and abbreviations

α	Flip angle (degree)
Δ	Time between the gradients
τ	Correlation time
ω	Larmor frequency
λ	Eigenvalue
γ	Gyromagnetic ratio
δ	Duration of gradient pulse
η	Viscosity
A	Signal attenuation
ADC	Apparent diffusion coefficient
AT	Acquisition time
b	Diffusion gradient dependent variable
B_0	Main magnetic field
c	Concentration
CSF	Cerebrospinal fluid
D	Diffusion coefficient
DT	Diffusion tensor
DTI	Diffusion tensor imaging
DWI	Diffusion weighted image
EPI	Echo planar imaging
f	Frequency
FA	Fractional anisotropy
FOV	Field of view
G	Gradient

GM	Gray matter
^{1}H	Hydrogen
IR	Inversion recovery
k	Boltzmann's constant
LCD	Laser Doppler flowmetry
M	Net magnetization vector
MCA	Middle cerebral artery
MCAO	Middle cerebral artery occlusion
MD	Mean diffusivity
MRI	Magnetic resonance imaging
MSME	Multi-spin multi-echo sequence
MTX	Matrix
M_t	The intensity of the detected magnetization
NA	Number of averages
NMR	Nuclear magnetic resonance
RF	Radio frequency
r_s	Stokes radius of the molecule
RMS	Root mean square
ROI	Region of interest
S	Signal at $b \neq 0$
S_0	Signal at b=0
SE	Spin echo pulse sequence
SNR	Signal to noise ratio
ST	Saturation recovery
St	Slice thickness
S(t)	Signal intensity

T2*	Effective transverse relaxation time, including signal reduction
T'_2	Inhomogeneity of the field B_0
T	Temperature
T1	Longitudinal relaxation time
T2	Transversal relaxation time
TR	Repetition time
TrD	Trace from tensor
t_{dif}	Diffusion time
WM	White matter

Contents

1 INTRODUCTION

Magnetic resonance imaging (MRI) has become an indispensable tool for disease diagnostics, especially in the brain. It is used widely in clinics and in research. With MRI it is possible to measure several distinct parameters non-invasively, without the flipside of radiation and priority; it can offer both good contrast between tissues according to desired determinant and several diagnostically relevant parameters.

Diffusion-weighted imaging (DWI) measures molecular mobility in one, predetermined direction. DWI is a sensitive tool for early identification and evaluation of ischemic stroke. It can detect the ischemic tissue in minutes after the stroke onset and later. As diffusion is really a three dimensional process, and the molecular environment can be anisotropic as it is in the brain white matter, a more recent method, called diffusion tensor imaging (DTI), can detect anisotropic diffusion. This way the existence of diffusion anisotropy can be extracted and characterized to gain more detailed data from the tissue microstructure.

The growing number of published DTI studies, show the great potential of the method. In the brain, DTI is a powerful tool for characterizing tissues, especially white matter (WM) structures, and tissue abnormalities caused by disease state. Especially, fractional anisotropy (FA, one of the DTI indices and a measure of anisotropic/ isotropic diffusion) was in focus in this study, since, it can offer unique information about the diffusion anisotropy. Most of the results that are available from diffusion anisotropy of the tissue after ischemic stroke are assessed by means of an orientation dependent parameter derived from ADC values, rather than from a rotationally invariant index derived from diffusion tensor (DT), such as FA. DTI is thought to depict the structural alignment and integrity of fibers and the changes in integrity after the stroke onset. In addition to that, it can distinguish white and gray matter infarction and acute from non-acute infarction. Still, the reported results from DTI after ischemic stroke are not uniform and sometimes even contradictory.

2 MAGNETIZATION

MRI is widely used in clinics because of its non-invasive and non-ionizing nature and because it can offer a diagnostically valuable contrast between tissues with good resolution. MRI contrast is rising from the difference in relaxation times or from the permeability between different tissues and / or normal and pathological tissue. That is why it would be useful to make an insight into the physico-chemical basis of NMR relaxation *in vivo*.

2.1 Physical principles of the phenomenon

MRI is founded on the principle of nuclear magnetic resonance (NMR). The principles of NMR are based on the ^{1}H (a proton), which is the most abundant isotope for hydrogen, and is present in high quantities in the human body (Brown, 2003). ^{1}H exhibits magnetism called a *magnetic moment* (Bushong, 2003). This means that if, for example, the human body is placed in a strong magnetic field, its H^{1}-nucleons will tend to line up with the field or opposite to it. This way the human body will become polarized. Polarization is presented in Figure 1 (Puddephat, 2005).

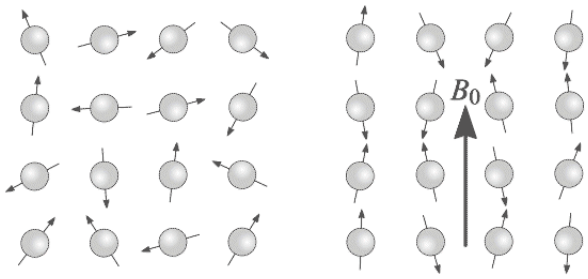

1) *Left: Under normal conditions proton are randomly oriented. Right: When a strong magnetic field B_0 is applied, the nucleons will line up with the field. (Puddephat, 2005)*

In addition to the polarization, there will also be precession of the protons when a strong magnetic field, B_0, is applied as shown in figure 2 (Puddephat, 2005). Proton has a quality known as *angular momentum*. The idea of an intrinsic *angular momentum* of the proton is fundamental to MRI. When a proton is spinning at an angle to the B_0, it will precess about the vertical axis (Figure 2). That is, the proton will rotate about its own axis, and the axis of the proton's rotation will revolve about the axis of B_0 (Figure 2). This precession is due to the angular momentum of the proton, which is again due to the natural spinning property of the proton.

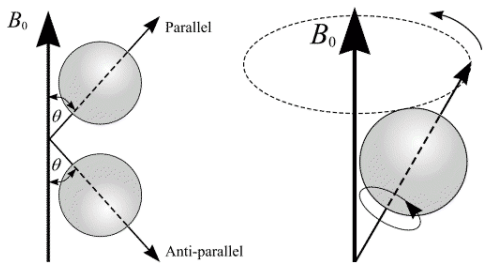

2) Left: In the presence of a strong magnetic field B0, nuclei will adopt one of two orientations with respect to B0. Right: A magnetic moment precessing around B0. (Puddephat, 2005)

The frequency at which the proton precesses is a function of both the strength of the magnetic field B_0 and the proton itself. This frequency in Larmor equation 1, called the *Larmor frequency*, is equal to the product of the strength of the magnetic field and a constant called the *gyromagnetic ratio* (γ). The *gyromagnetic ratio* is unique for each nucleus for ^{1}H proton it is 42.6 MHz/T (Brown, 2003). The *Larmor frequency* is the frequency at which the proton will absorb energy that will cause it to change its alignment.

$$\omega = \gamma B_0 \qquad (1)$$

When radio frequency (RF) energy is applied with the *Larmor frequency*, the protons, which aligned with the B_0, will absorb energy and reverse their direction. Over a period of time the protons will relax back to their original alignment with the magnetic field. When protons are relaxing, they will emit energy whose frequency is the *Larmor frequency*. There are two different ways how protons relax called T1 relaxation and T2 relaxation.

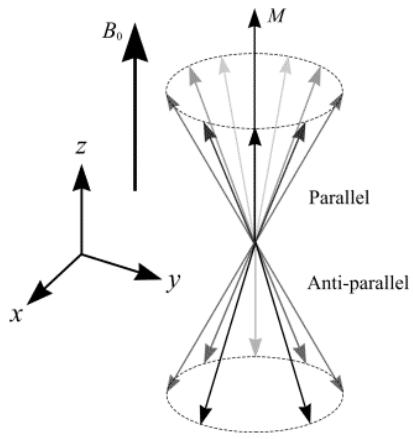

3) As slightly more nuclei align along than opposite with the strong magnetic field B_0, a small net magnetization, M, is detectable in the direction of B_0. (Puddephat, 2005)

Slightly more protons align in the direction of the magnetic field B_0 than the opposite direction, creating a small net magnetization effect (*M*), which can be easily understood as the sum of the contributions of all the *magnetic moments* of the individual protons as seen in a figure 3 (Puddephat, 2005).

2.2 Relaxation

After the RF pulse, the net magnetization vector will eventually return to its equilibrium status. The recovery of magnetization to the z-axis is termed longitudinal and the time constant for this process is T1. The other form of relaxation, covering the gradual loss of transverse magnetization, is characterized by a time constant T2. Bloch equations present these procedures (Equation 2 and 3) (Bloch, 1946):

$$\frac{dM_z(t)}{dt} = \frac{M_0 - M_z(t)}{T_1} \tag{2}$$

$$\frac{dM_{xy}(t)}{dt} = -\frac{M_{xy}(t)}{T_2} \tag{3}$$

Where M_0 is the equilibrium magnetization and M_z and M_{xy} are magnetization components along z axis in the xy plane. Note that the signal decays exponentially.

As the equations 2 and 3 show, relaxation results from time-dependent fluctuations of magnetic fields. Several parameters affect the fluctuating magnetic field; translational motion of molecules (diffusion), molecular rotations generating fields at the nucleus (rotation), chemical exchange, and fields generated by unpaired electrons. These mechanisms can only cause relaxation when there is a time-dependent interaction at an appropriate time scale because only field fluctuation at specific frequencies can evoke relaxation. This dependence on relaxation times can be described according to equations 4 and 5:

$$\frac{1}{T_1} = K\left[\frac{\tau_c}{1+\omega_0^2\tau_c^2} + \frac{4\tau_c}{1+4\omega_0^2\tau_c^2}\right] \tag{4}$$

$$\frac{1}{T_2} = \frac{K}{2}\left[3\tau_c + \frac{5\tau_c}{1+\omega_0^2\tau_c^2} + \frac{2\tau_c}{1+4\omega_0^2\tau_0^2}\right] \tag{5}$$

Where, $K = 3\mu_0^2 \hbar^2 \gamma^4 / 160\pi^2 r^6$ (γ = gyromagnetic ratio, μ = magnetic dipole moment, $\hbar = h / (2\pi)$ where *h* is Planck's constant and r is the radius) is a constant and τ is correlation time that describes the time at which the given physical factors can influence spin behavior. From the equations 4 and 5 it is possible to conclude that T1 is sensitive to processes occurring about the Larmor frequency whereas T2 is more sensitive in lower frequencies.

The recovery of the net magnetization is caused by the fluctuating magnetic field emerging from the motion of molecules in the neighborhood of the magnetic moments. Therefore, the T1 and T2 recovery rates can tell about the mobility of the molecules (particularly water molecules) and hence the binding of water molecules.

2.2.1 T1 measurement

A common method to measure the T1 is the so-called inversion recovery (IR) sequence (figure 4), in which the net magnetization is first inverted to the - z-axis. The net magnetization will gradually return back to the + z-axis at rate determined by T1. A 90 degree pulse is applied after given time periods following the inversion to read the z magnetization acquired, and thus to monitor the longitudinal relaxation. The time period between the inversion pulse and the 90-degree pulse is called the inversion time, TI. The intensity of the detected magnetization (M_t) is presented in equation 6.

$$M_t = M_0(1-2e^{(-TI/T_1)}) \tag{6}$$

M_0 is the net magnetization at the equilibrium. By repeating the experiment with several TI values, T1 can be calculated by fitting signal intensities to the equation.

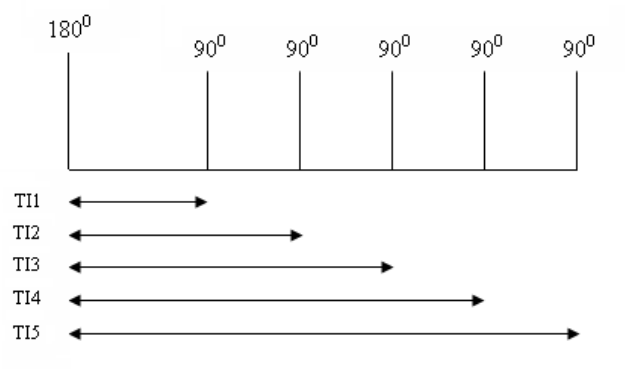

4) IR sequence for measuring T1 is presented

IR sequence is commonly used for measuring T1. It is an accurate way of measuring T1, but the imaging time can be fairly long because of the repeats with different TI values. There are several ways to measure T1; such as variants of the IR sequence, the saturation recovery sequence (SR) (figure 5), the stimulated echo sequence, the look-locker sequence, and many others. In this work, I use SR sequence that is presented in figure 5. This technique is quicker than an IR sequence but is still considered accurate. SR sequence consists of multiple 90 degree RF pulses at relatively short repetition times (TR). The signal will reflect T1 differences in tissues because of different amounts of longitudinal recovery during the TR. By fitting the signal intensity data with each TR, T1 can be calculated as the equation 7 presents.

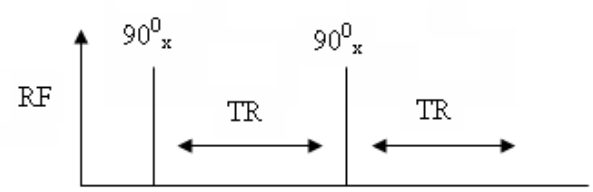

5) A saturation recovery sequence has 90^0 RF pulse after time of repetition TR.

$$M_t = M_0(1 - e^{(-TR/T_1)}) \quad (7)$$

M_t is the intensity of the detected magnetization, M_0 is the net magnetization at equilibrium, and TR is the repetition time.

In normal tissue T1 values are related to macromolecule concentration, water binding, and water content. This is the reason for the basic T1 contrast in the brain: myelin causes white matter to have a shorter T1 than gray matter.

2.2.2 T2 measurement

Analogous to T1, T2 is called the transverse relaxation time. T2 relaxation time represents the interference from equilibrium, which is the xy magnetization. Everything that will affect to relaxation of M_z will also affect the relaxation of the M_{xy}. Anyhow, there are also supplementary processes that will only affect the relaxation M_{xy} and hence T2. This will characterize processes in which T2 is equal to or shorter than T1 in biological samples.

Net magnetization vector (M) consists of several protons and they all behave independently although they altogether form the net magnetization. Therefore each proton will experience a slightly different magnetic field because of their environment. Individual protons will lose their coherence, which is called dephasing. Dephasing will lead to random phase disruption and therefore to the loss of the detectable net magnetization in *xy*-plane. Reason for the dephasing can be static inhomogeneities or interactions between individual spins. Static inhomogeneities can rise from instrumental imperfection of the main field B_0 or from susceptibility differences within sample. Because of the instrumental imperfections, the field inhomogeneity within the sample is always present. It means that some individual protons will experience slightly different local magnetic field than their neighbors. Magnetic susceptibility is a measure of the extent in which a sample can modify B_0 (Brown, 2003). In addition to static inhomogeneities, intramolecular and intermolecular dipolar interactions cause dephasing. To summarize all these dephasing processes, there is a time constant T_2* that takes into consideration all these variables in equation 8:

$$\frac{1}{T_2^*} = \frac{1}{T_2} + \frac{1}{T_2'} \quad (8)$$

where T'_2 is the relaxation time constant due to static field inhomogeneity.

The part of which static field inhomogeneities are removed and T2 relaxation time constant can be measured by using a spin-echo sequence (Gröhn, 2003), which is presented in figure 6. In spin echo sequence a 180-degree pulse is applied at a predefined time following the 90-degree pulse. 180-degree pulse will reverse the phases of the protons. As the rates and the direction of the precession of the protons remain the same, protons will regain their phase coherence at the time point matching the delay between 90 and 180-degree pulses. The reformed coherence will induce NMR signal called the spin-echo. The time from the 90-degree pulse to the maximum intensity of spin-echo is called the echo time, TE. The detected magnetization (M_t) is presented in equation 9.

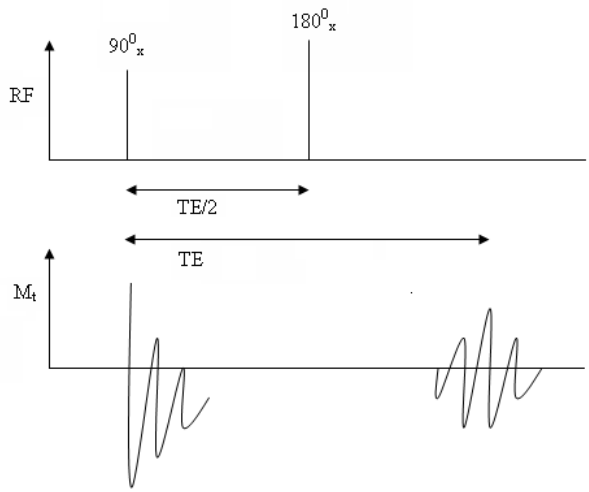

6) A spin echo experiment generates a detectable echo at a time TE after the 90^0 RF pulse.

$$M_t = M_0 e^{(-TE/T_2)} \tag{9}$$

T2 time constant can be measured from signal intensities measured with variable echo times. In the Carr-Purcell multi-echo sequence, T2 is measured by having a train of refocusing pulses as seen in figure 7.

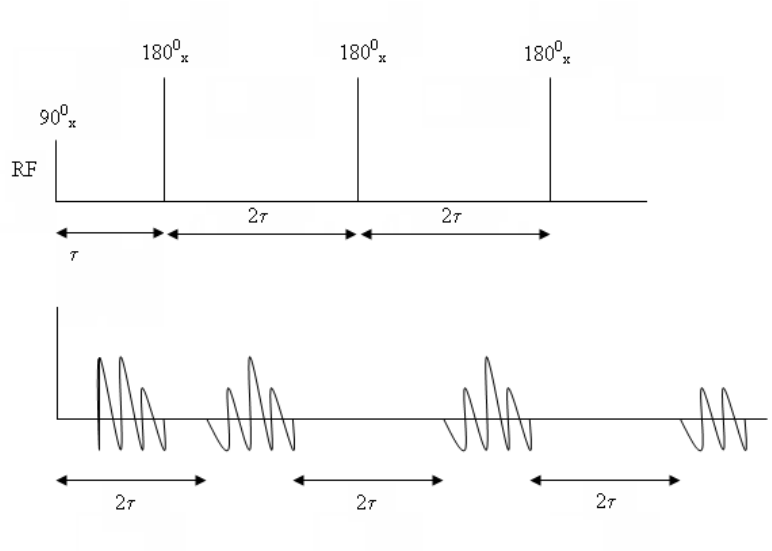

7) Cascade of 180^0 pulses can be used to generate a spin echo train. The echo will decay because T2 star is present. The time 2τ is equal to TE.

3 DIFFUSION

3.1 Diffusion and self-diffusion

Diffusion is general transport of matter whereby molecules or, which is driven by Brownian motion (Brown, 1827). Each molecule within the sample behaves independently from the others. The collision between molecules provokes a random displacement of each one, without a preferred direction. This phenomenon is called *the random walk* and is presented in Figure 8. When given a time interval, t_{dif}, it is possible to calculate a statistical measure of diffusion distance, D (*diffusion coefficient*), averaged over an equilibrium ensemble of molecules, the so-called *root mean square* (RMS) distance.

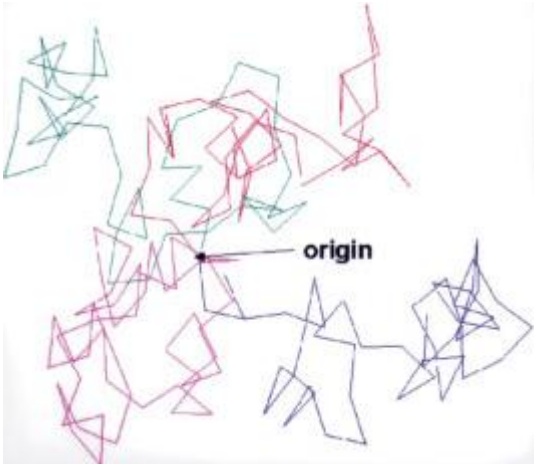

8) This is representation of the random walk. Line presents the origin of the walk (Beaulieu, 2002)

By using Einstein equation (1-dimensional RMS = $(2D\ t_{dif})^{1/2}$) it is possible to calculate the diffusion constant, D, but it is impossible to say in what direction or how far a single given molecule has moved during time, t_{dif}. For example free water molecules diffusing in water at 37 °C, the D is 3 $x10^{-9}$ m^2s^{-1}, which comes from diffusion distance of 17 µm during 50 ms (Le Bihan, 2006).

The factors influencing diffusion in a solution are molecular weight, intermolecular interactions (viscosity), and temperature as the equation 10 presents. Equation 10 is called the Stokes-Einstein equation (Beaulieu, 2002).

$$D = \frac{kT}{f} = \frac{kT}{6\pi\eta r_s} \tag{10}$$

where k is the Boltzmann constant, T is the temperature (Kelvin), f is the friction coefficient (which is proportional to the Stokes radius of the molecule, r_s), and η is the viscosity of the solution.

Even though the diffusion motion is a random process, there is an underlying driving mechanism. When describing the mixing of two different liquids or gases, diffusion is usually described in terms of the concentration gradient of the diffusing substance. In biological tissues, however, concentration is not the driving force, and the process of interest is instead the motion of water within water, driven by thermal agitation, and referred to as *self-diffusion*.

3.2 Restricted diffusion

In human tissues, the water molecules are constantly in random motion because of their thermal energy (Brown, 1827). Water diffusion in vivo is affected by the micro dynamics of cellular transport between different subcompartments of the heterogeneous tissue structure as well as by the presence of nonpermeable membranes. Because such obstacles affect the movement of water molecules, the actual diffusion distance is reduced compared with that of free water. The path of a single water molecule is, therefore, directly depending on structure of its microenvironment. Because the intracellular space contains more obstacles than the extracellular space, the diffusion is more restricted in the intracellular space. Indeed, this is a microscopic phenomenon but when large amounts of molecules are involved, it gives rise to a macroscopically observable and measurable phenomenon. As a conclusion, the non-invasive follow up of the diffusion-driven displacement distributions in vivo provides unique insight into tissue structure and organization, potentially giving information about the size, orientation, and complexity of both the intra- and extra-cellular spaces. It can also reveal changes in the tissue in physiological and pathological stages when water compartments between intra- and extra-cellular spaces will change.

3.3 Diffusion transport of magnetization and dMRI

The image intensity can be made sensitive to many parameters relating to the microenvironment of the tissue. In addition to T1 and T2, MRI can be made sensitive to the diffusion of water molecules, which can reveal the condition of the tissue. This is done by pulse sequence alterations; generating a set of pulse sequences adapted to acquire DWI (Stejskal and Tanner, 1965).

DWI is based on the spin echo sequence with extra encoding process. Both of these imaging methods are presented in Figure 9 (Roberts and Schwartz, 2007). The difference is that, a short, high-amplitude gradient pulse is applied between 90- and 180-degree pulse and after the 180-degree refocusing pulse. In the presence of this gradient any molecular displacement occurring during the time between first and second gradient (Δ) produces a phase shift of the signal (diffusion weighted spin echo). Due to the very large number of water molecules present in the tissue, the phase shifts are distributed, reflecting the diffusion-driven displacement distribution, resulting in a loss of coherence, and hence, an attenuation of the MRI signal.

For measuring ADC_i (diffusion-sensitizing gradient is applied in direction *i*), only two points with a different *b*-values is needed: one at a very low *b*-value (zero is

often used) and another at a high *b*-value (in clinical applications *b* = 600 -1500 s/mm^2 (Mukherjee et al., 2008a):

$$ADC_i = -\ln(S_i / S_0) / b \quad (11)$$

where ln is the natural logarithm. The signal intensity S_0 in the absence of a diffusion-sensitizing gradient (image with *b* = 0 s/mm^2) and S_i in the presence of diffusion-sensitizing gradient (image with the high *b*-value).

While knowing the ADC of the tissue, a simple rule of thumb is that the optimal *b*-value multiplied by the ADC of the tissue under investigation should be close to 1 (Mukherjee et al., 2008b).

As the equation 12 shows, parameter "*b*" reflects the sensitivity of the imaging sequence to the process of diffusion. For gradient pulses, *b*-value can be derived from the gyromagnetic ratio (γ), amplitude (G), duration (δ), and time between the gradients (Δ) (Le Bihan, 1990):

$$b = \gamma^2 G^2 \delta^2 (\Delta - \delta / 3) \quad (12)$$

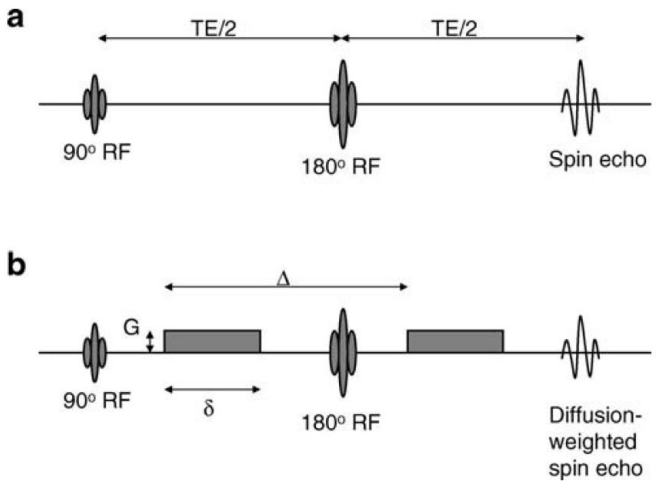

9) ***a****: Spin echo formed by combination of 90^0 and 180^0 RF pulses (time between the pulses is TE/2)* ***b:*** *By adding two gradients (G), it will result as a spin echo plus DW spin echo (reduced echo). (Roberts and Schwartz, 2007)*

Effect of increasing *b*-value can be seen in Figure 10, where on the left side *b* = 0 s/mm^2, in the middle *b* = 500 s/mm^2, and on right side *b* = 1500 s/mm^2. By increasing the *b*-value, lesion can be depict easier but with the expense of SNR (Roberts and Schwartz, 2007). On the other hand, some have reported how the signal intensity of brain water shows non-monoexponential decay when measuring with high *b*-values (Niendorf et al., 1996, Mulkern et al., 1999, Clark and Le Bihan, 2000,

Brugieres et al., 2004). Because there is a limit for the gradient amplitude strength, to obtain larger *b*-value, the other compartments should be increased in the equation 12. On the other hand, by increasing either duration of the pulse or time between the pulses, it will increase the TE (increase T2-weighting).

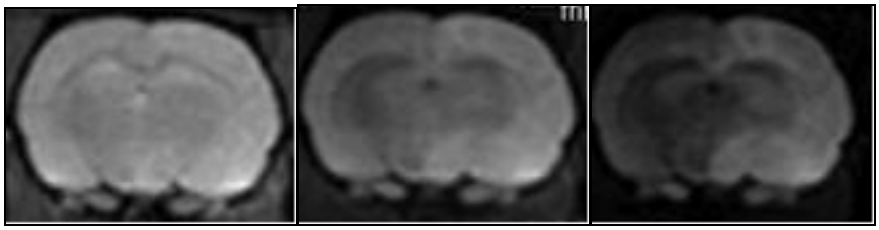

10) left: b=0 s/mm^2 (T2W), middle: b=500 s/mm^2, right: b=1500 s/mm^2.

4 DIFFUSION TENSOR IMAGING

Measurement of the signal attenuation from water diffusion is one of the most important contrast mechanisms in MRI. As diffusion is a three-dimensional process, molecular mobility in tissues may not be equal in all directions. DTI may be used to map and characterize the three-dimensional diffusion of water as a function of spatial location (Basser et al., 1994a, Basser et al., 1994b). Diffusion anisotropy was first observed in brain white matter (Moseley et al., 1990). Before that, most information about structural anatomy of the white matter has been acquired through post mortem analysis. At the moment, DTI can provide unique *in vivo* information about white matter structural anatomy and cerebral connectivity (Roberts and Schwartz, 2007).

Diffusion anisotropy in white matter originates from its construct in bundles of axonal fibers. Diffusion in the direction of the fibers (longitudinal to the fibers) is faster than to the other directions (perpendicular to the fibers). Diffusion anisotropy is a measure of the directional dependence of the diffusion restriction. WM is an example of anisotropic environment and contrary to that, cerebrospinal fluid (CSF) would be a good example of isotropic environment. In isotropic environments, water diffuses equally in all directions. GM is considered more isotropic than WM (Beaulieu, 2002).

4.1 dMRI measures diffusion only in one predetermined axis

A DW image is created by applying a pair of magnetic field gradients (dephasing and rephasing gradients) along a distinct direction in 3D space. The resulting image, therefore, shows signal attenuation in the direction of the applied gradient and this signal attenuation is directly proportional to water diffusion. For example, by applying a gradient in one direction (x, y, or z in the coordinate system), information from water motion in that single direction will be acquired. By combining three directions (x, y, and z), the ADC along the most notable directions can be measured. In figure 11, measurements in three different directions are presented. As the figure 11 shows, the contrast in each direction is different; z-direction shows higher diffusion in cortical areas than two other directions. When the diffusion is not the same in all directions, it is called anisotropic diffusion.

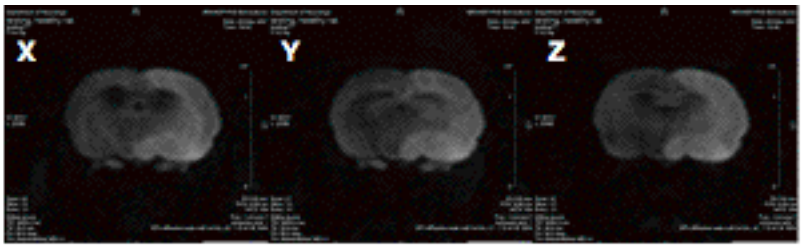

11) ADC measurement is presented in three different directions (x, y and z). It can be noticed that the diffusion is not similar in all directions.

Even if three measurements in three different orientations (x, y, and z) would be averaged, yet it would not suffice to make an accurate measurement of diffusion. This is because fibers do not strictly go along one of these orientations. Basser et al (Basser et al., 1994a) presented earlier the concept of DT. In this model, measurements in several directions are fitted to 3D shape. The properties of the 3D shape are the length of the longest, middle, and the shortest axes (called eigenvalues) and their orientation (called eigenvectors).

4.2 DT measures diffusion in 3D

The diffusion tensor can be visualized three-dimensionally as the diffusion ellipsoid. In this ellipsoid presentation, the eigenvectors define the direction of the principal axes and the eigenvalues the dimensions of the ellipsoid.

To define a perfect sphere, only one parameter is needed, which is the diameter of the sphere as seen in figure 12a (Roberts and Schwartz, 2007). An oval would need three parameters to be identified; two parameters for the length of the long and short axis and one parameter to define the orientation of one of the axis. For defining an ellipsoid, six parameters would be needed; three lengths for the longest, shortest and middle axes, and one parameter to define the orientation of all these axis. These three axes are perpendicular to each other in ellipsoid as seen in figure 12b (Roberts and Schwartz, 2007). When talking about diffusion tensor, we need to define the eigenvalues that can be divided in order of decreasing magnitude (λ_1 = highest diffusivity, λ_2 = intermediate diffusivity, and λ_3= lowest diffusivity). As seen in figure 12b, eigenvalues are the three principal coefficients measured along the three orientations and each eigenvalue is linked with a principal direction, eigenvector.

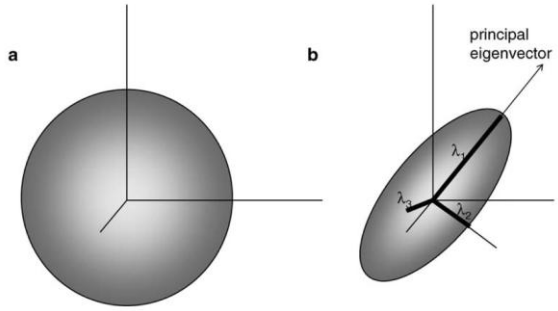

12) a: Isotropic environment can be considered as a sphere. b: For defining anisotropic diffusion, three eigenvalues $\lambda_1, \lambda_2, \lambda_3$, and principal eigenvector are needed. This is ellipsoid presentation of diffusion tensor. (Roberts and Schwartz, 2007)

Diffusion tensor ellipsoid can take several forms depending on the eigenvalues as seen below in figure 13. Figure 13A presents the case when eigenvalues are equal and this will be seen as a sphere. This environment can be found for example in CSF where diffusion is isotropic. When the three eigenvalues are not equal, we can have multiple variations of the shapes (for example in figure 13B and 13C there are two possible shapes). Most areas of the WM are more or less anisotropic which results in

variable unbalance between the eigenvalues (compare B and C). Meanwhile GM is considered as a more or less isotropic environment, and CSF is isotropic.

The eigenvalue magnitudes will be affected by changes in local tissue microstructure in many types of tissue changes; disease, tissue destruction, and development of the tissue after birth or aging. Thus, DT can trace for both normal and abnormal processes in the tissue.

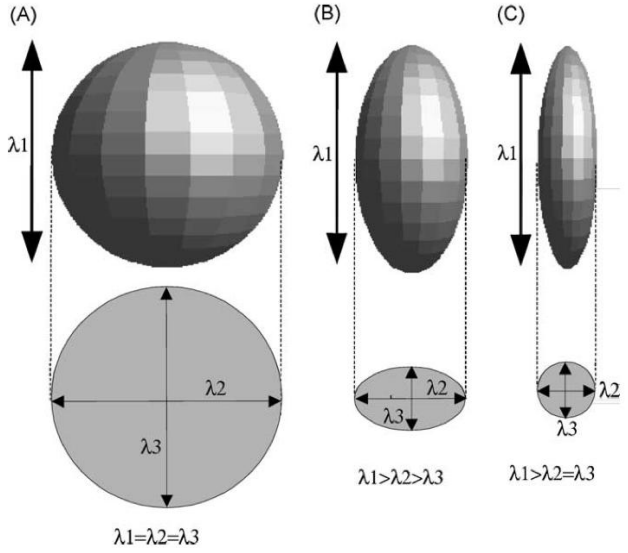

13) This is ellipsoid representation of the diffusion tensor with the eigenvalues λ1, λ2, and λ3. Three different environments for the diffusion in presented; (A) represents isotropic environment and (B)/(C) represents different anisotropic environments. (Mamata et al., 2004)

4.3 Mathematical presentation of DTI

In the presence of anisotropy, diffusion can no longer be characterized by a single scalar coefficient, but requires a tensor, DT. DT describes molecular mobility along each direction and correlation between these directions. In equation 13, tensor is a symmetric and positive definite 2.-order tensor which can be presented as a 3×3 matrix:

$$DT = \begin{bmatrix} D_{xx} & D_{xy} & D_{xz} \\ D_{yx} & D_{yy} & D_{yz} \\ D_{zx} & D_{zy} & D_{zz} \end{bmatrix} \quad (13)$$

where $D_{xy} = D_{yx}$, $D_{xz} = D_{zx}$, $D_{yz} = D_{zy}$, and therefore DT contains six elements. For isotropic diffusion, the off-diagonal elements of DT are all zero and the diagonal elements are equal, like in equation 14. In this case the diffusion process could as well be described by a single scalar, D:

$$D = DT\begin{bmatrix} 1 & 0 & 0 \\ 0 & 1 & 0 \\ 0 & 0 & 1 \end{bmatrix} \tag{14}$$

In isotropic environment, there is no preferred direction of molecular motion. In contrast, for an anisotropic environment the molecular mobility varies and depends on the orientation of the medium.

Diffusion often occurs in the system, where there is a flux of a certain type of particles (water molecules). This can be described using Fick's law:

$$j = -DT \cdot \nabla C(r,t) = -\begin{bmatrix} D_{xx} & D_{xy} & D_{xz} \\ D_{yx} & D_{yy} & D_{yz} \\ D_{zx} & D_{zy} & D_{zz} \end{bmatrix} \begin{bmatrix} \frac{\partial C(r,t)}{\partial x} \\ \frac{\partial C(r,t)}{\partial y} \\ \frac{\partial C(r,t)}{\partial z} \end{bmatrix} \tag{15}$$

where *C(r,t)* is the particle concentration, $\nabla C(r,t)$ is the concentration gradient, and *j* is the particle flux density. The minus sign in equation 15 indicates that the diffusing mass flows in the direction of decreasing concentration.

Instead of using equation 15, it is more useful to present the diffusion as a distribution function (equation 16). Assume that we can mark a diffusing water molecule located at position 0 at time *t = 0*. The general form of this distribution function is presented in equation 16. Figure 14 shows a projection of the probability changes when it is measured in different time points. In equation 16, the probability of finding a water molecule at time t at position r is *f (r, t)*:

$$f(r,t) = \frac{1}{\sqrt{|DT|(4\pi t)^3}} \cdot e^{-(r^T DT^{-1} r)/4t} \tag{16}$$

where | DT | is the determinant of the DT.

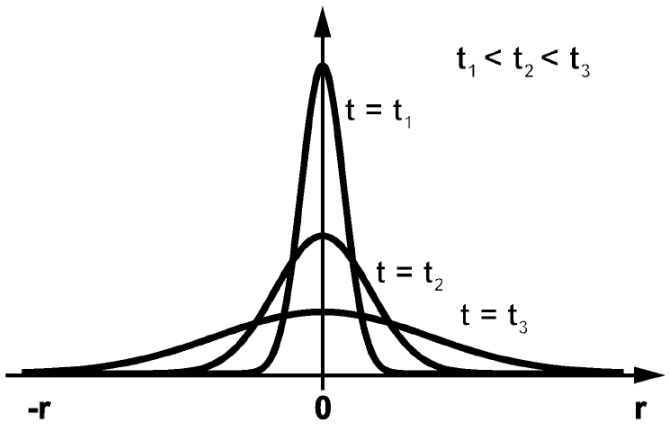

14) Probability distributions of finding a water molecule at different locations at time t = t1, t2 and t3. (Skare, 2002)

4.4 Rotationally invariant measures derived from DTI

Once DT is obtained, it should also be visualized to detect the anatomical structures of the brain. In addition to visualization, we need to achieve scalars for quantitative measurements. The two most common ways to do this is the mean diffusivity (MD) and the fractional anisotropy (FA) map. Specifically, these measures are independent of the orientation of both tissue structure and the image scan plane. This is referred to as rotational invariance. Rotational invariance means that the same intensity for the same anatomical location regardless of the orientation of the tissue and of the image scan plane.

4.4.1 Mean diffusivity

The average of the three eigenvalues of the ellipsoid can be considered as a "scale factor" of the diffusion ellipsoid. This is referred to as mean diffusivity (MD) and will be hereafter being denoted as ADC. To calculate MD from the diffusion tensor one can simply average the eigenvalues of DT as seen in equation 17.

$$MD = \frac{\lambda_1 + \lambda_2 + \lambda_3}{3} = \frac{TrD}{3} \tag{17}$$

In standard DWI, the gradient is applied in x-, y-, or z-direction. This is seen in equation 18. In equation 19, "≈" means that mean ADC (⟨ADC⟩) can be slightly different from MD.

$$\langle ADC \rangle = \frac{ADC_x + ADC_y + ADC_z}{3} \tag{18}$$

$$\langle ADC \rangle \approx MD \tag{19}$$

MD is similar in WM and GM despite the fact that the diffusion is isotropic in GM and anisotropic in WM.

4.4.2 Diffusion anisotropy

Basser et al (Basser and Pierpaoli, 1996) originally presented the fractional anisotropy (FA) index (equation 21). FA is easily understood as the extent of which the ellipsoid can get in different environments as seen in figure 15. Figure 15 shows that eigenvalues ($\lambda_1 > \lambda_2 > \lambda_3$) and eigenvectors ($e_1$, e_2 and e_3) determine the 3D ellipsoid. DTI ellipsoid is presented in equation 20 and in figure 15.

$$\frac{x'^2}{2\lambda_1 T} + \frac{y'^2}{2\lambda_2 T} + \frac{z'^2}{2\lambda_3 T} = 1 \tag{20}$$

where T is diffusion time (also seen in Figure 15).

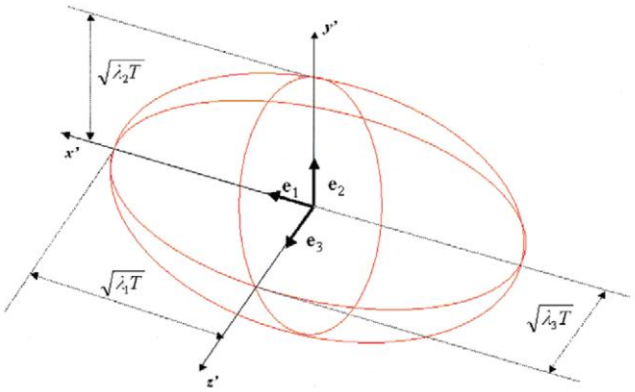

15) Ellipsoid of directional anisotropy. The surface of the ellipsoid represents the distance of molecule motion from the origin in a certain diffusion time (T). (Masutani et al., 2003)

Several diffusion anisotropy indices have been proposed in the literature. Common to all of them is that the anisotropy index should depend on how anisotropic the diffusion is, i.e. how much the diffusion ellipsoid deviates from sphere. At the same time, anisotropy indices should be independent of the orientation of the diffusion ellipsoid- rotational invariant.

Still, FA does not describe the full tensor shape as seen from the equation 21. This is because different combination of λ_1, λ_2, and λ_3 can give the same value of FA. Still, FA is thought to be adequate enough for many applications and appears to be sensitive to a wide range of pathological conditions (Alexander et al., 2007):

$$FA = \sqrt{\frac{3}{2}} \sqrt{\frac{(\lambda_1 - \bar{\lambda})^2 + (\lambda_2 - \bar{\lambda})^2 + (\lambda_3 - \bar{\lambda})^2}{\lambda_1^2 + \lambda_2^2 + \lambda_3^2}} \tag{21}$$

where $\bar{\lambda} = \frac{\lambda_1 + \lambda_2 + \lambda_3}{3}$

FA is widely used to differentiate between anisotropic and isotropic tissues (Roberts and Schwartz, 2007). From the equation 21 it can be noticed that FA could have values from 0 to 1, where 0 presents absolute isotropy and 1 presents full anisotropy. This can also be seen in figures 16 (healthy) and 17 (2 days after the stroke), where the ischemic tissue appears dark after the stroke onset in FA image. As the white arrow in figure 17 points out, the corpus callosum is clearly damaged after the ischemic stroke.

MD is also presented in healthy (Figure 16, right) and in ischemic brain (Figure 17, right).

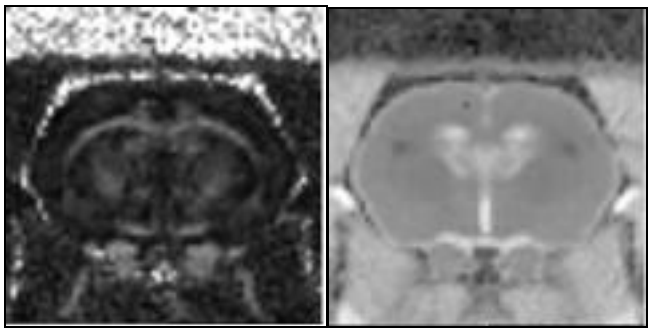

16) Left: gray scale FA of a healthy brain. Anisotropic tissues appear white and present highly oriented white matter tracks. Right: gray scale MD of the same animal. There is no visual difference between isotropic and anisotropic tissues while isotropic CSF appears bright.

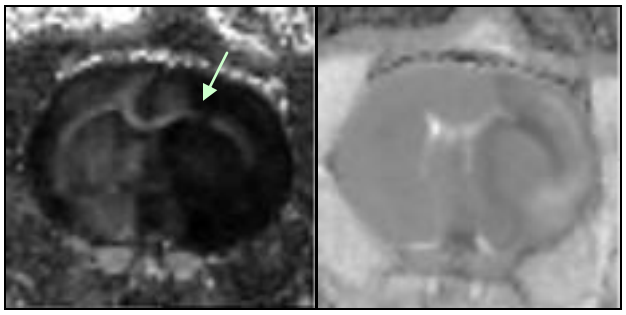

17) Left: gray scale FA of an ischemic brain 48h after stroke onset. Ischemia is in the right hemisphere. Disruption of corpus callosum is pointed out with the arrow. Right: gray scale MD of an ischemic brain 48h after stroke onset. Ischemia is in the right hemisphere.

5 DT IMAGE QUALITY AND ARTIFACTS

5.1 Multi-shot and single-shot EPI

Pulse sequences can be divided into multi-shot (acquires several excitations to fill the k-space) and single-shot (acquires only a single excitation to fill the k-space) pulse sequences. Multi-shot sequences provide a good resolution, image contrast, and SNR with scan times usually of few minutes. A problematic issue of multi-shot acquisition is the need to ensure that different acquisition "shots", for a given image, undergo similar degree of motion artifact. Another issue that should be considered is that images that are sensitive to different direction of motion are not differentially affected.

DTI sequences usually require relatively long imaging times. While using multi-shot sequence with DTI, troublesome ghosting artifact, caused by patient motion, can appear. In single-shot sequence the image is acquired in seconds, and ghosting artifacts do not appear. Still, the multi-shot approach is shown to offer data with good precision and accuracy, despite the flipside of the ghosting artifact.

5.2 Essential variables that affect the DT sequence

There are some basic requirements for clinical applications of DTI. For example, the total scan time should not be too long, relatively thin sections are required for accurate recognition of structures, and a sufficient number of sections are needed to cover the whole brain. Optimization of the DTI acquisition protocols is needed by taking into consideration the above requirements.

One of the most important factors in DTI acquisition is the number of diffusion-encoding directions (NDGD) (Ni et al., 2006). A number of studies (Jones et al., 1999, Papadakis et al., 1999a, Papadakis et al., 1999b) have shown that for a given number of DW images, the use of more than six NDGDs improve the measurement of D. When number of NDGDs increases, more DW images are used for calculating D, and as a result, more accurate D (and simultaneously more accurate FA, ADC, λ_1, λ_2 and λ_3) estimation results. When the scanner hardware has improved rapidly in recent years, use of more NDGDs has become popular. Papadakis et al (Papadakis et al., 2000) presented that the minimum number of encoding directions required for robust anisotropy estimation is between 18 and 21. A more recent study concluded that at least 20 NDGDs are needed for robust estimation of anisotropy and 30 NDGDs were needed for a robust estimation of tensor orientation and mean diffusivity (Jones, 2004, Ni et al., 2006).

Alternatively, more averaging (larger NA) of each DW image also results in a higher SNR and better estimation of D. By increasing either NA or NDGD, it will result in a longer imaging time, and because sequences are designed for clinical use, the imaging time should be kept as short as possible. However, it is reported that one

should use as many NDGDs as the imaging time allows (Jones, 2004). Hence, there is still no consensus about different combination for choosing of the amount of NDGDs and NA for the evaluation of DTI indices (Ni et al., 2006).

Fixation of the patient is very essential in in-vivo DTI studies where motion contamination can significantly disturb the measurement. Ni et al (Ni et al., 2006) underlined the importance of minimizing the movement during the DTI. In addition to other motion, there is some movement rising from the venous pulsation. Even if it is very minor, this pulsation can disturb the sequence. This arises from the fact that DW sequence is sensitive to water diffusion within the measurement time (t_{dif} in Einstein equation) and brain pulsation motion can be larger than water diffusion. Within the brain, the timing of data acquisition relative to the cardiac cycle has recently been shown to influence the quality of DTI studies and cardiac triggering is recognized as a good solution- both with brain- and spinal cord-DTI (Dietrich et al., 2000, Summers et al., 2006). Still, some find the use of cardiac triggering not necessary and explain it as being needed only in a time when the systems had low spatial resolution- nowadays systems offer higher spatial resolution and different pre- and post -reconstructions are done to the image (Robson and Porter, 2005).

5.3 Ischemic stroke and DTI - previous works

When looking at the previous DT studies with ischemic stroke, not all of these studies scanned individual patients/animals at each time point to control between subject variability, and many have only few sampling time point when following the evolution of ischemic stroke (Carano et al., 2000, Lee et al., 2006, Liu et al., 2007). Especially, when making a follow up study with patients, it is not possible to know the exact time of the stroke and this way the time points are never accurate enough to compare with laboratory circumstances. Also, patient studies are difficult to categorize between transient and permanent group. Permanent ischemia models mimic human stroke without recanalization, which is minority of human ischemic stroke (therapy-induced recanalization) (Durukan and Tatlisumak, 2009). As a result, patient studies can be a mixture of transient and permanent ischemia patients and the comparison between patient and animal study can be arguable.

The scanning protocols are always optimized to compromise between scanning time and image outcome (Chapter 5.2). There is a range of studies that have NDGDs from 6 to 32 and with different NA, which will result as multiple variable SNRs and resolutions between the studies. Therefore, results are not directly comparable. A study performed by Bastin et al (Bastin et al., 1998) demonstrated that the dependence of ADC on SNR was relatively weak. In contrast, RA and simultaneously FA ($FA = \sqrt{(3(RA^{-2} + 2)^{-1})}$) was significantly increased when the SNR was reduced below 20. This threshold should be paid attention to when comparing the results. Another variable that can cause variability between the studies is the scanner. With predetermined imaging time, High-field (~ 3.0T - 11.0T) animal scanners can offer higher SNR, as well as a stronger magnetic gradient, which enables a better resolution compared to clinical MR scanners (~ 1.5T – 3T).

6 APPLICATION STUDIES WITH DTI

DTI has become one of the most popular MRI techniques in brain research, as well as in clinical practice. This methodology has been used to study the architecture and integrity of the intact and diseased brain (stroke, multiple sclerosis, aging, dementia, schizophrenia, etc.) DTI can provide image contrast that is not available with routine MR techniques, unique information on white matter, and visualization of neuronal pathway in 3D.

DTI can offer several indices for measuring the contribution and movement of the water in a unique way. Figure 18 summarizes the main indices (FA, ADC, λ_1, λ_2, and λ_3) that can be extracted from the DTI image and analyzed further. Myelin is unique to white matter and is therefore believed to be one of the main sources of the DTI signal. Because of this, almost every disease where myelin is reduced (multiple sclerosis, etc.) or disturbed (stroke, etc.), can be searched with this method. The absence of myelin appears as a reduction of diffusion anisotropy. Figure 18 also shows how the value of FA (measure of diffusion anisotropy) decreases as the ischemia evolves over the time and the tissue injury increases. In the same figure, the other indices have their own characteristic way to change while they all carry individual data about diffusion. In addition to stroke, DTI has been applied to other brain diseases. Lim et al (Lim and Helpern, 2002) reported neuropsychiatric applications of DTI; such as alcoholism, geriatric depression, and schizophrenia. Outside the brain, it is more difficult to use DTI because of its sensitivity to movement. Still, there exist studies done outside the brain. For example, there are applications with the skeletal muscle (Morvan, 1995), breast (Englander et al., 1997), and liver (Namimoto et al., 1997). Still, most of the published DTI studies are related to brain tissue or brain connectivity. Especially DTI tractography is bringing a totally new dimension while it is the only method for tracking the brain white matter fibers noninvasively.

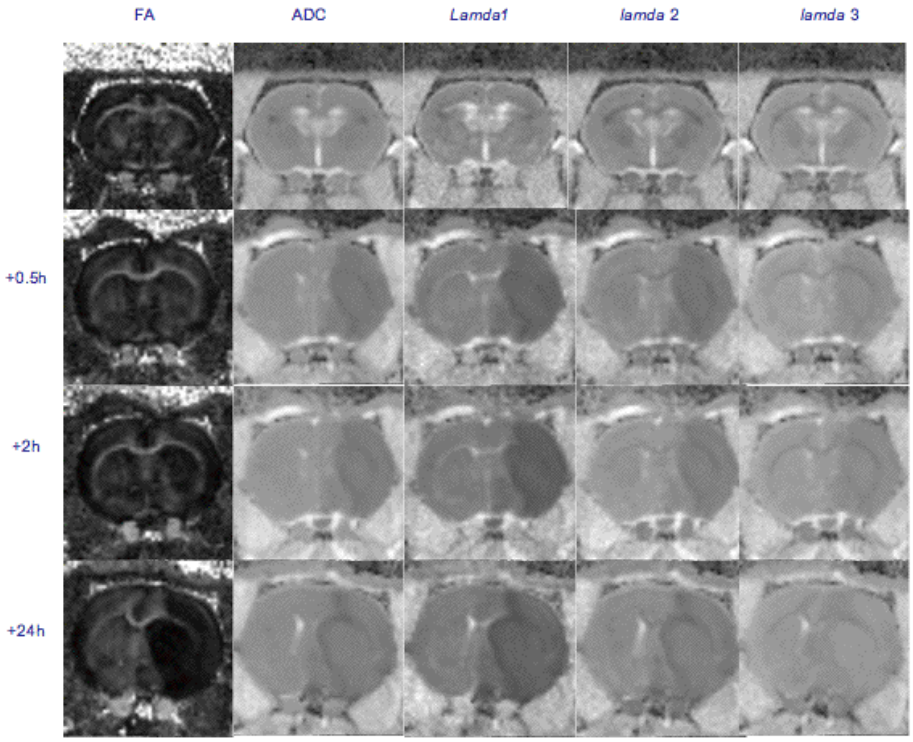

18) *The first row represents diffusion tensor indices of a healthy animal. The next rows represent the same indices 0.5 hour, 2 hours, and 24 hours after ischemia. (unpublished data)*

7 ISCHEMIC STROKE

7.1 Ischemic stroke in humans

Stroke is the third most common cause of death after cancer and heart disease and the most common cause of disability in people over 60 years of age (Rantanen and Tatlisumak, 2004, Emre et al., 2007, Tatlisumak et al., 2007). Over 700,000 strokes come up every year alone in the United States causing to over 200,000 deaths (Thom et al., 2006). Stroke absorbs a big slice of all health budgets being ~ 6% in the United Kingdom (Rothwell, 2001). In United States, the annual costs are 40 billion USD (Broderick et al., 1998). Clearly, the stroke patients are a big burden for the healthcare system. To relieve some of this burden, an effort should be done towards early detection and therapy of stroke. The identification of the causes, duration, localization, and severity of ischemia in early phase is necessary to prevent massive tissue injury. Two major current treatment options are trombolysis and neuroprotection (Durukan and Tatlisumak, 2007). Early diagnosis and appropriate treatment can prevent the tissue to evolve into infarction (Tatlisumak, 1999).

MRI is an efficient tool for depicting changes in the brain tissue caused by ischemia. It works as an indispensable tool in stroke research for two major purposes: evaluation of ischemic lesion in all phases of the stroke and assessment of drug efficacy after the medication (Fisher and Tatlisumak, 2005).

7.2 Animal model

Ischemic stroke is an individual clinical state. There are several variables that can change between individual patients; the cause of the stroke, duration, localization in the brain, and severity of ischemia (Durukan et al., 2007a). Patients can also have co-existing diseases. All of these variables can be present, and take part to the progress of the infarction. Clinical research requires very large patient groups to minimize the contribution of these variables and to gain appropriate statistical power. To conclude, clinical stroke studies in the human are difficult to carry out, expensive, and time consuming (Durukan et al., 2007a). To mimic these human studies, experimental animal models have been developed. Animal models have several advantages compared to human studies; ischemia can be physiologically well controlled, and will eliminate most of the unwanted variables. Rat is the most commonly used animal for studying experimental brain ischemia. Rat stroke models have played a unique role in understanding the changes caused by ischemia (Durukan and Tatlisumak, 2007).

Ischemia is defined as a reduction in brain blood flow severe enough to cause tissue damage. The reduction in blood circulation is usually abrupt and due to a vascular arterial occlusion. Borderline ischemia is considered to exist when blood circulation is reduced to less than about 50% of control (Tatlisumak, 1999). To mimic this reduction of the blood flow that happens due to ischemia, one of the vital arteries of

the brain has to be blocked. One of the most popular methods is the middle cerebral artery occlusion (MCAO) that is seen in figure 19. MCAO is done by transiently blocking the arterial flow with a removable suture, or by permanently occluding the artery by leaving the suture in place (Koizumi et al., 1986).

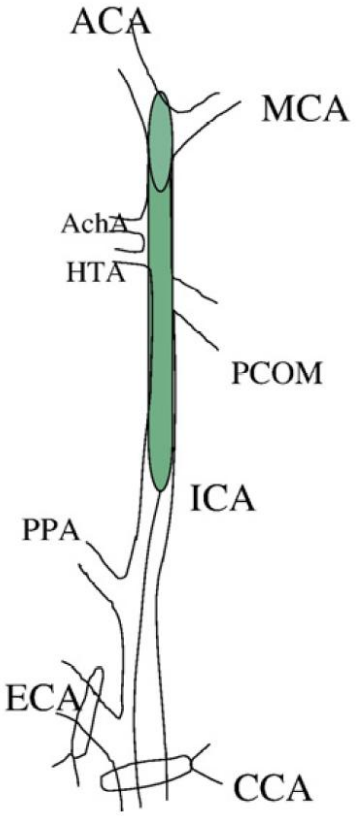

19) Middle cerebral artery occlusion (MCAO) is done by transiently or permanently blocking the arterial flow with a suture. Surrounding arteries are also presented as abbreviations. (Durukan et al., 2007b)

7.3 Brain ischemia: central core and penumbra

The goal of stroke therapy is to protect brain tissue before irreversible injury develops. A transition from reversible to irreversible injury is dependent on the severity and the duration of ischemia (Pearson, 1896). It is known that reversible ischemic tissue progresses towards infarction (Pearson, 1896). A central core with severely deducted blood flow is thought to be surrounded by a rim of milder ischemic tissue. This rim is called “penumbra” and it can have variable outcome. Outcome depends on several factors, duration of vessel occlusion being the most determinant. The data that has been published, characterizes the ischemic core and penumbra in both human and in rodent stroke. The term “brain ischemia” includes both infarct core and brain penumbra.

7.4 Detection of different phases with MR

Cerebral ischemia evolves in three phases/stages after the stroke onset. There is a cascade of events that takes place in different time points as seen in figure 20. From these phases it can be distinguished that an acute phase of stroke (< 24 hours), a sub-acute phase (3-5 days), and a chronic phase (occurring within days to months) exist (Rodriguez-Yanez et al., 2006).

All three phases has own mechanisms to occur as figure 20 presents. According to earlier publications, acute phase can be defined by several characteristic phenomena; movement of water from extracellular space to intracellular space (Warach et al., 1992), decreasing membrane permeability (Helpern, 1992), decreasing in cytoplasmic circulation (Wick et al., 1995), and cell swelling (van der Toorn et al., 1996). In the subacute and chronic phases of stroke, the vasogenic edema and the subsequent disruption of the cytoarchitecture will occur and finally the programmed cell death will be activated (Carano et al., 2000, Rodriguez-Yanez et al., 2006).

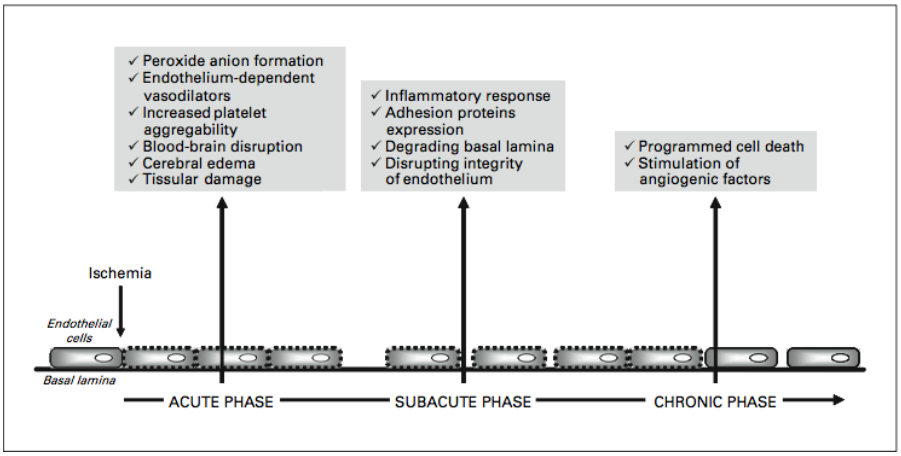

20) The mechanisms of damage after the stroke. Three phases can bee differentiated after the stroke: acute, subacute and chronic phase. (Rodriguez-Yanez et al., 2006)

MR parameters can reflect these different phases of the cascade; distinguish acute infarcts from non-acute infarcts and demonstrate how the ischemia evolves (Mintorovitch et al., 1991, Chien et al., 1992, Helpern, 1992, Warach et al., 1992, Davis et al., 1994, Warach et al., 1995, Welch et al., 1995, Marks et al., 1996, Lutsep et al., 1997, Armitage et al., 1998, Yang et al., 1999, Zelaya et al., 1999). Especially DTI indices such as ADC and FA can reflect the condition and environment of water molecule in a more advanced way.

The temporal evolution of water ADC and diffusion anisotropy in human stroke are similar to that observed in rodent models (Zelaya et al., 1999, Carano et al., 2000). Some have reported that the evolutions of events that take place after the ischemic stroke are much slower in humans than in rodents (Liu et al., 2007).

ADC decreases immediately after the onset of acute cerebral ischemia, which is followed by renormalization and later increase in ADC during the chronic phase (Mintorovitch et al., 1991, Chien et al., 1992, Knight et al., 1994, Warach et al., 1995, Lutsep et al., 1997, Schlaug et al., 1997, Schwamm et al., 1998, Ahlhelm et al., 2002). In acute and subacute phases, increase in diffusion anisotropy has been observed (Mintorovitch et al., 1991, Armitage et al., 1998, Yang et al., 1999), although some have reported decrease (Zelaya et al., 1999). Remarkable changes happen in diffusion anisotropy during the sub-acute and chronic phases when diffusion anisotropy decreases strongly (Zelaya et al., 1999, Carano et al., 2000, Munoz Maniega et al., 2004). This is logical since diffusion anisotropy reflects the presence of intact cell membranes and myelin fibers and as the ischemia proceeds the loss of structural integrity also proceeds. In chronic phase (> 90 days) the value of diffusion anisotropy increases which for example might be due to the development of glial scar tissue as the infarct resolves (Carano et al., 2000, Sakail, 2007).

7.5 WM and GM in human and in rodent brain

The GM consists of neuronal cell bodies, their dendrites, and axons, plus glial cells and blood vessels. The WM consists mostly of bundles of axons, glial cells and blood vessels. Only small amount of myelin exist in the GM, whereas it is abundantly present in the WM.

To recall, that when comparing human brain and rodent brain, it should be considered that the ratio of WM and GM is different in human and in rodents; as the brain size increases, the volume of the WM beneath the cortex increases faster than the volume of the cortical GM alone. In rodents, WM constitutes only about 14% of total brain volume while in human, WM totals to about 50% of the brain volume (Muir and Grosset, 1999, Zhang and Sejnowski, 2000).

7.5.1 WM and GM have distinct patterns of change after ischemic stroke

Many studies have reported different response of FA in WM and GM after the ischemic stroke; both in patients (Yang et al., 1999, Munoz Maniega et al., 2004) and in animal studies (Carano et al., 2000). Maniega et al and Yang et al (Yang et al., 1999, Munoz Maniega et al., 2004) reported that FA of WM tissue decreased more rapidly than FA of GM tissue after the stroke onset in patients. In contrary, Carano et al (Carano et al., 2000) reported stronger decrease of FA in cortex than in subcortex in rats.

Different evolution of ADC in ischemic WM and GM has also been reported (Sorensen et al., 1999, Bastin et al., 2000). Sorensen et al (Sorensen et al., 1999) reported significantly lower values of ADC in ischemic WM than in ischemic GM. Bastin et al. (Bastin et al., 2000)observed earlier ADC-renormalization in ischemic GM than in ischemic WM.

The changes in water apparent diffusion are thought to be related to changes in brain water content. Changes in anisotropy are linked to changes in tissues microstructure. In the gray matter, this may reflect changes in the dendritic architecture of pyramidal cells. In the case of white matter, this is due to changes in the myelination.

Different neuronal structure between WM and GM make it possible that the mechanism of ischemic injury and strategies for protection will vary. This way, FA and ADC may allow separate evaluation of the treatment response of WM and GM to neuroprotective therapy.

7.5.2 T1- and T2- relaxation times after the ischemic stroke

In earlier studies it has been reported that T1 and T2 change within minutes after the onset of ischemia and reach to a maximum at the early days after the onset (Kettunen et al., 2000, Makela et al., 2002). Relaxation times decrease thereafter, and stabilize or increase again slightly over the next weeks (Ishii et al., 1998, Li et al., 2000a, van Dorsten et al., 2002). T1 and T2 relaxation times are sensitive to an increase in free, extracellular water, such as in vasogenic edema. After the stroke onset and later, water is thought to gather in the brain once the blood brain barrier (BBB) is disrupted and the increase in overall water content is believed to cause the changes in T1 and T2 (Kato et al., 1986, Mintorovitch et al., 1991, Naruse et al., 1991).

The temporal and spatial behavior of T1- and T2- relaxation times has been shown to be different from the behavior of ADC and FA, which is related to their different origin (Helpern et al., 1993, Hoehn-Berlage et al., 1995). This might offer a different view when following the evolution of ischemia.

8 MATERIALS AND METHODS

8.1 Animals and surgical procedures

Adult male Wistar rats (Harlan Nederland, Horst, The Netherlands), weighting 250 to 400 grams, with free access to food and water and kept at 12/12 h light/ dark cycle, were anesthetized by an intraperitoneal injection of ketamine hydrochloride (50 mg/kg, Ketalar, Parke-Davis, Detroit, MI) and subcutaneous injection of medetomidine hydrochloride (0.5 mg/kg, Domitor, Orion, Espoo, Finland). During the surgery, body temperature was maintained at 37° C. Middle cerebral artery occlusion (MCAO) was used (Koizumi et al., 1986). The suture MCAO model was used to induce either permanent (n = 9) or transient (n = 9) ischemia (Tatlisumak et al., 1998). A nylon suture was inserted into the internal carotid artery. In the group with transient MCAO, reperfusion was accomplished by withdrawing the occluder after 90 minutes of ischemia. The success of MCAO and reperfusion was confirmed with LCD (Laser Doppler flowmetry). All experiments were performed in conformity with the institutional guidelines and national and international laws and international policies for use of animals in neuroscience research. The local Animal Research Committee had approved the study protocol.

8.2 The imaging protocol

The MRI measurements were performed with a 4.7 T MR Scanner (PharmaScan, Bruker, Germany) designed for experimental animals. The coil was a dedicated rat head coil (Bruker linear birdcage coil, gradient strength 300 mT/m, and rise time < 80 µs). Experiment is started by placing the animal into the animal bed. The head is fixed in a holder with tooth and ear bars to avoid movement during the imaging. First, MR Scanner performs shimming (pre-adjustments). Shimming is followed by a Scout-sequence that localizes the brain. Scout image is used for choosing the suitable anatomic landmark where the multi slice imaging pack is placed. Careful alignment of the imaging pack enhances the reproducibility of the images between individual animals and time points.

Wistar rats were subjected to focal cerebral ischemia by suture occlusion of MCA for 90 minutes followed by reperfusion (n = 9), or permanent occlusion (n = 9). They were imaged 2 and 3.5 hours, 1, 2, 3, and 4 days, 1, 2, 4, 6, and 8 weeks after the MCAO. Sham-operated rats were used as healthy controls (n = 8). During imaging, the respiration rate of the rat was monitored using respiration sensor (external signal synchronization, Bruker Biospin, Germany) and body temperature was maintained within physiological ranges with a heating pad.

The multi-spin multi-echo sequence (MSME), based on CPMG (Carr-Purcell Meiboom-Gill) spin echoes (SE) was used for T_2–weighted imaging and determination of T_2 [repetition time (TR) = 1500 ms, echo time (TE) = 10 - 320 ms and 32 echoes, number of averages (NA) = 2, matrix (MTX) size = 256 x 192, field-

of-view (FOV) = 40 x 40 mm, single slice with slice thickness (St) = 2.0 mm, acquisition time (AT) = 7min 12s].

T_1-relaxation time was obtained by a fast spin-echo saturation-recovery sequence. [TR = 150, 300, 600, 1500, 3000, and 4500 ms, effective echo time TE = 56 ms, NA = 2, MTX = 128 x 128, FOV = 40 x 40 mm, single slice with slice thickness St = 2.0 mm, acquisition time AT = 5min 21s, RARE factor = 8].

Diffusion tensor (DT) indices were acquired from multi-shot spin-echo echo-planar image (EPI) with 30 NDGDs [TR = 3000 ms, TE = 35 ms, Δ = 20 ms, δ = 4 ms, b =1500 s/mm^2, NA = 2, MTX = 128 x 128, FOV = 40 x 40 mm, single slice with St = 2.0 mm, AT = 14 min].

To consider T1 measurements accurate, I compared my results from SR sequence to those obtained from IR sequence and the result was uniform. Results were also compared to published data of T1 and T2 measurements and the results were similar (for 4.7 T system and human brain T1: GM = 1459 ±11 ms, WM = 1312 ± 14 ms (Kettunen et al., 2000) and T2: GM = 65.9 ± 1.1 WM = 55.8 ± 2.2 ms (Loubinoux et al., 1997)).

8.3 Region of interest analysis

DWI hyperintensity was observed in the right MCA region already at the first time point (2 hours after ischemic stroke), involving either only subcortical or cortical regions, but mainly both. The acute temporal evolution of diffusion tensor indices (ADC and FA), T1, and T2 were evaluated by the absolute mean values and afterwards by calculating the ratios between ischemic tissue and its contralateral counterpoint region (abbreviations for the ratios are rADC, rFA, rT1, and rT2). The mean values of diffusion tensor indices, T1, and T2 were calculated for the regions of interest (ROI) located in the cortex, subcortex and in corpus callosum (corpus callosum is a heterogeneous WM tract that connects the cerebral hemispheres) regions as the figure 21 presents. For the selected slice, three ROIs were placed to the most affected tissues by infarction. For comparison, I selected mirror regions for the healthy hemisphere.

The results are presented as ratios to control the homogeneity. A comparison between the absolute value and ratio value was done and the evolution of the values and the statistics were found to be fairly similar. In the earlier works, there seems to be a general agreement to use ratios instead of absolute values (Oppenheim et al., 2001).

Lesion areas were calculated by measuring the lesion area manually from DWI up to day 1 and from T2WI after that. To achieve the lesion volume, the measured lesion area was multiplied by the slice thickness.

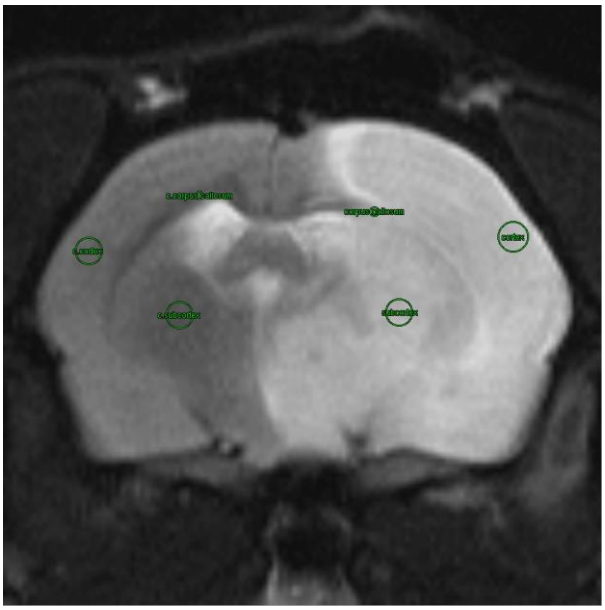

21) The placement of the ROIs is presented in T2-weighted image, 1week after MCAO. There are three ROIs in each hemisphere; in subcortical, cortical and in corpus callosum area. ROIs are placed manually but approximately to the area with the highest signal intensity in the ischemic hemisphere.

8.4 Data adjustment

Distortions of EPI sequence are generated by main magnetic field inhomogeneities; susceptibility differences between the tissue and the air. The manufacturer has included several automatic adjustments that can improve the image. ParaVision includes a special utility for EPI reconstruction off-line, called freco (BrukerBiospin Para Vision, EPI reconstruction off-line) (Hennel, 1998). This freco uses a special algorithm to derive the linear correction coefficient and applies this correction to all repetitions. When freco is used for reconstruction, it takes into consideration adjustments of the acquisition delay (between slices and motion related) and the preemphasis (gradient waveform and timing).

8.5 Statistical analysis

Data are presented as mean ± standard deviation (SD). Normally distributed parametric data sets in multiple groups were compared with one-way analysis of variance (ANOVA) followed by the Holm-Sidak post-hoc test. The question answered by the one-way ANOVA test is whether group means differ from the control group mean of cortex, subcortex, and corpus callosum in the contralateral counterpoint region when it was compared to the same regions in the healthy animals.

With Student's t-test I did: 1) a comparison between cortex, subcortex, and corpus callosum in all time points (2 hours- 8 weeks), 2) comparison between transient and permanent MCAO in cortex, subcortex, and corpus callosum in all time points (2

hours- 8 weeks), and 3) comparison between lesion volumes in transient and permanent ischemia. Values were considered statistically significant if $P < 0.05$.

9 RESULTS

9.1 ADC and FA in healthy subjects

The result (first row) from eight healthy animals and some results from the other most recent DTI works are given in Table 1. When FA and ADC of cortex, subcortex, and corpus callosum were compared, FA showed significant difference between the tissues ($p < 0.001$), and ADC no significant difference between the tissues ($p > 0.05$). T1 and T2 showed significant difference between corpus callosum and cortex / subcortex ($p < 0.001$), but not between cortex and subcortex ($p > 0.05$) (data not presented).

Table 1. Absolute values of ADC and FA in different brain regions. These results are obtained from healthy animals / volunteers. Regions are described as subcortical, cortical, and corpus callosum regions in the present study. Other studies reported their results from white matter (WM), grey matter (GM), or from corpus callosum. Standard deviation (SD) is in brackets and ADC x10^{-3} mm^2/sec.

subject, (NDGD)	*Reference*	*Subcortex, ADC*	*Subcortex, FA*	*Cortex, ADC*	*Cortex, FA*	*Corpus callosum, ADC*	*Corpus callosum, FA*
rat, (30)	*Our results*	*0.64(0.03)*	*0.30(0.07)*	*0.67(0.04)*	*0.19(0.06)*	*0.62(0.10)*	*0.44(0.09)*
		WM	*WM*	*GM*	*GM*		
rat, (32)	*(Lee et al., 2006)*	*0.63(0.03)*	*0.32(0.09)*	*--*	*--*	*0.64(0.01)*	*0.31(0.10)*
rat, (6)	*(Kim et al., 2008)*	*0.69(0.05)*	*0.48(0.09)*	*1.92(0.09)*	*0.23(0.07)*	*--*	*--*
human, (6)	*(Le Bihan et al., 2001)*	*0.64(0.03)*	*--*	*0.83(0.05)*	*--*	*0.69(0.05)*	*--*
human, (6)	*(Sorensen et al., 1999)*	*0.72(0.05)*	*0.37(0.04)*	*0.62(0.07)*	*0.84(0.04)*	*--*	*--*
human, (12)	*(Ward et al., 2006)*	*0.62(0.02)*	*0.16(0.07)*	*--*	*--*	*--*	*--*
human, (6)	*(Munoz Maniega et al., 2004)*	*0.96(0.03)*	*0.14(0.01)*	*0.83(0.02)*	*0.43(0.02)*	*--*	*--*
human, (6)	*(Guilfoyle et al., 2003)*	*--*	*--*	*--*	*--*	*--*	*0.58(0.04)*
human, (6)	*(Price et al., 2005)*	*--*	*--*	*--*	*--*	*0.89(0.10)*	*0.74(0.09)*
human, (6)	*(Zelaya et al., 1999)*	*--*	*0.52(0.06)*	*--*	*0.23(0.05)*	*--*	*0.85(0.06)*

9.2 Results after permanent MCAO

9.2.1 Ratio of ADC and FA

The absolute values of FA and ADC from ischemic and contralateral side are presented in appendix A (Table A1). The values of ADC and FA in normal appearing hemisphere are not significantly different from the healthy animals throughout the observation period (2 hours – 8 weeks) ($p > 0.05$).

rADC of subcortical regions is significantly different from the normal at all the time points except at 4w and 6 w ($p < 0.001$) (figure 22 (a)). In the cortical regions, rADC is significantly different from the normal at time points 2h, 3.5h, 1d, 6w, and 8w ($p < 0.01$) (figure 22 (b)). In the corpus callosum regions, rADC is significantly different from the normal over the time period from 2 hours to 1 week ($p < 0.05$) (figure 22 (c)). After MCAO, the maximum decrease of rADC is 51 % in subcortex (at 3.5h), 39 % in cortex (at 3.5h), and 58 % in corpus callosum (at 2h) of the initial value. After the decrease, rADC starts to increase steadily and normalizes about 4 weeks in subcortex, 2 weeks in cortex, and 2 weeks in corpus callosum. Afterwards, rADC increases steadily up to 6 weeks in all tissues (figure 22). In table 2, it was tested whether there is a difference in rADC between the tissues at each time point.

rFA of the subcortical regions is significantly different from the normal over the time period from day 1 to 4 weeks ($p < 0.04$) (figure 22 (a)). Cortical regions are significantly different from the normal (healthy animal) over the time period from day 2 to1 week ($p < 0.03$) (figure 22 (b)). In the corpus callosum regions, rFA is significantly different from the normal at a time point 2d ($p < 0.03$) (figure 22 (c)). The decrease after the MCAO is most pronounced in the cortical region where rFA-value decreases 67 % (up to 4 days) of the initial value, while subcortical and corpus callosum regions decrease less (subcortical regions decrease 61 % (up to 2 days) and corpus callosum regions 34 % (up to 2 days)). In table 2, it was tested whether there is a difference in rFA between the tissues at each time point.

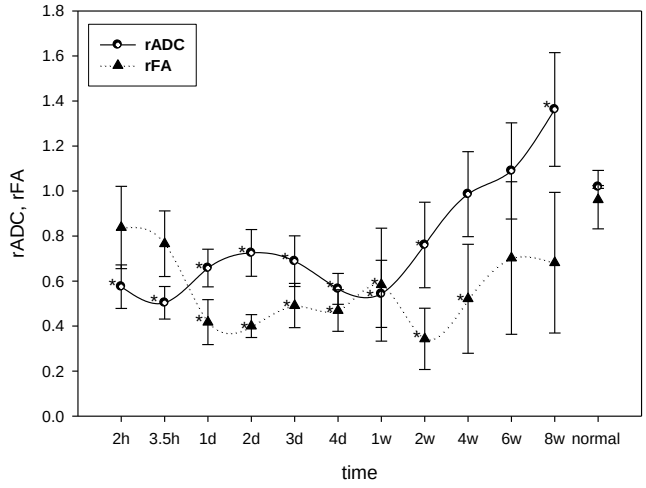

a)

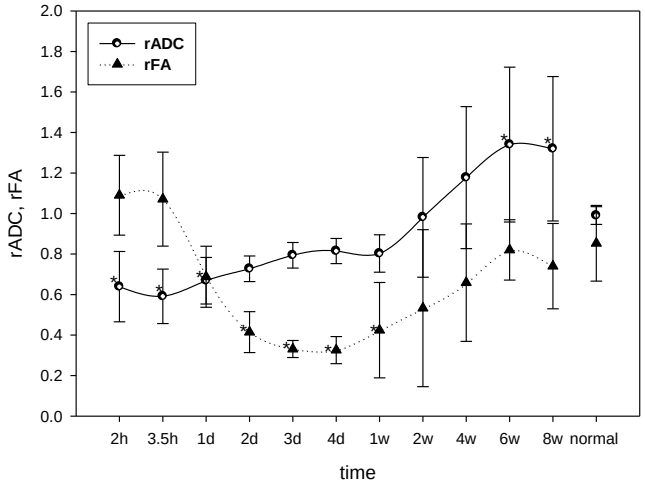

b)

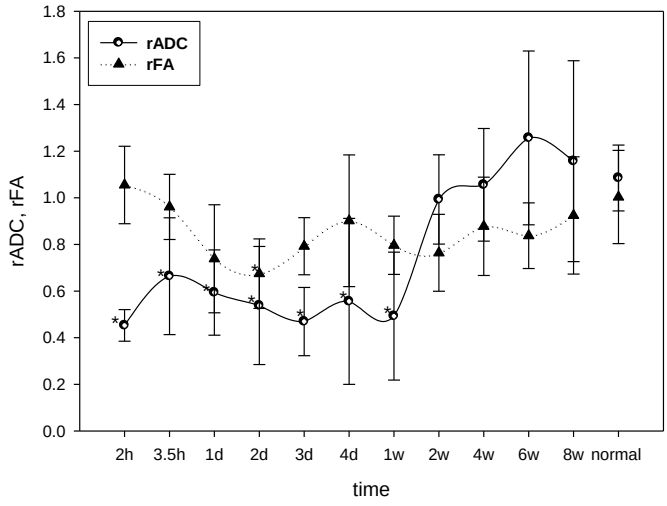

c)

22) a) (subcortex), b) (cortex), and c) (corpus callosum): Each point is a ratio between ischemic tissue and their contralateral position. The evolution of DTI indices, rFA and rADC, over 8 weeks (2 hours – 8 weeks), is presented for subcortex, cortex, and corpus callosum. Normal presents the ratio between healthy right and left hemisphere in healthy animals. Time points that are significantly different from the normal are marked with an asterisk (*). In the a) (subcortex) (*) stands at 2h, 3.5h, 1d, 2d, 3d, 4d, 1w, 2w, 8w (rADC). In the b) (cortex) (*) stands at 2h, 3.5h, 1d, 6w, 8w (rADC) and 2d, 3d, 4d, 1w, 2w (rFA). (*). In the c) (corpus callosum) (*) stands at 2h, 3.5h, 1d, 2d, 3d, 4d, 1w (rADC) and 2d (rFA).

Table 2. Table presents the t-test results. Tissue parameters (rADC and rFA) are compared at each time point during the 8 weeks observation period (2h, 3.5h, 1d, 2d, 3d, 4d, 1w, 2w, 4w, 6w, and 8w after MCAO). Significantly different time points are presented with their p-values.

PERMANENT ISCHEMIA	
rADC	
cortex vs. subcortex	***3d (p = 0.03), 4d (p<0.001), 1w (p =0.003)***
corpus callosum vs. cortex	***2h (p = 0.012), 3d (p < 0.01), 1w (p = 0.014)***
corpus callosum vs. subcortex	***2h (p = 0.011), 3d (p = 0.006)***
rFA	
cortex vs. subcortex	***2h (p = 0.02), 3.5h (p = 0.006), 1d (p < 0.001)***
corpus callosum vs. cortex	***2d (p = 0.003), 3d (p < 0.001), 4d (p < 0.001), 1w (p = 0.015)***
corpus callosum vs. subcortex	***2h (p = 0.039), 3.5h (p = 0.013), 1d (p = 0.003), 2d (p = 0.011), 3d (p < 0.001), 4d (p = 0.003), 4w (p = 0.022)***

9.2.2 Ratio of T2 and T1

The absolute values of T2 and T1 from ischemic and contralateral side are presented in appendix A (Table A2). The values of T2 and T1 in normal appearing hemisphere are not significantly different from the healthy animals throughout the observation period (2 hours – 8 weeks) ($p > 0.05$).

rT2 is significantly different from the normal at time points 1d, 2d, 3d, 4d, 2w, 4w, 6w, 8w (cortex, $p < 0.02$), 2w (subcortex, $p < 0.03$), and 4d (corpus callosum, $p < 0.03$) (figure 23 (a)). 2 hours after MCAO, rT2 of cortical and subcortical regions increases and reaches the first maximum at 1-2 days. The first maximum is followed by the second peak at 2-4 weeks. After the second peak, rT2 stays high while comparing to the normal. Corpus callosum has only one maximum at the fourth day, during the 8 weeks observation period. After that fourth day, rT2 of corpus callosum decreases steadily to the level of the normal. In table 3, it was tested whether there is a difference in rT2 between the tissues at each time point.

rT1 is significantly different from the normal at the late time points 4w, 6w, 8w (cortex, $p < 0.01$), 2w, 4w, 8w (subcortex, $p < 0.02$), while corpus callosum is not significantly different from the normal at any time point (figure 23 (b)). Up to 4 days after the MCAO, rT1 of cortical and subcortical regions is higher than the normal and later rT1 increases steadily until it becomes significantly different from the normal. Afterwards, rT1 stays significantly different from the normal in cortical and subcortical regions. In table 3, it was tested whether there is a difference in rT1 between the tissues at each time point.

Table 3. Table presents the t-test results. Tissue parameters (rT2 and rT1) are compared at each time point during the 8 weeks observation period (2h, 3.5h, 1d, 2d, 3d, 4d, 1w, 2w, 4w, 6w, and 8w after MCAO). Significantly different time points are presented with their p-values.

PERMANENT ISCHEMIA	
rT2	
cortex vs. subcortex	***1w (p = 0.003), 2w (p = 0.049)***
corpus callosum vs. cortex	***2h (p = 0.026), 1d (p < 0.001), 4w (p = 0.003), 6w (p < 0.001), 8w (p < 0.001)***
corpus callosum vs. subcortex	***2h (p = 0.019), 1d (p < 0.001), 4w (p = 0.014)***
rT1	
cortex vs. subcortex	***1w (p = 0.011)***
corpus callosum vs. cortex	***4w (p = 0.02), 8w (p = 0.049)***
corpus callosum vs. subcortex	***3.5h (p = 0.019), 4w (p = 0.022), 8w (p = 0.036)***

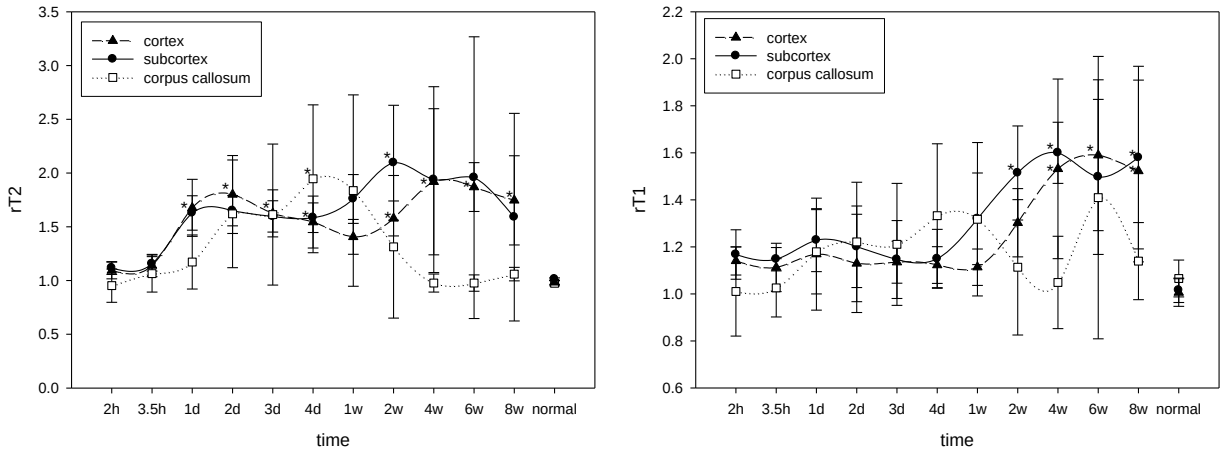

a) ***b)***

23) (rT2) and b) (rT1): Each point is a ratio of ischemic tissue and their contralateral position. The evolution of rT2 and rT1, over 8 weeks (2 hours – 8 weeks), after permanent MCAO, is presented for subcortical, cortical, and corpus callosum regions. Normal presents the ratio between healthy right and left hemisphere in healthy animals. Time points that are significantly different from the normal are marked with an asterisk (*). In the a) (rT2) (*) stands at 1d, 2d, 3d, 4d, 2w, 4w, 6w, 8w (cortex), 2w (subcortex), and 4d (corpus callosum). In the b) (rT1) (*) stands at 4w, 6w, 8w (cortex), 2w, 4w, 8w (subcortex).

9.3 Results of transient MCAO

9.3.1 Ratio of ADC and FA

The absolute values of FA and ADC from ischemic and contralateral side are presented in appendix B (Table B1). The absolute values of ADC and FA in normal appearing hemisphere are not significantly different from healthy animals in throughout the observation period (2 hours – 8 weeks) ($p > 0.05$).

rADC of subcortical regions is significantly different from the normal at time points 2h, 3.5h, 1d, 2d, 4w, 6w, and 8 week ($p < 0.03$) (figure 24 (a)). In the cortical regions, rADC is significantly different from the normal at the time points 4w, 6w, and 8w ($p < 0.01$) (figure 24 (b)). In the corpus callosum regions, rADC is significantly different from the normal at a time point 3.5h ($p < 0.04$) (figure 24 (c)).

At the first time point (2 hours after MCAO), rADC drops 41 % (at 3.5h) in subcortex, 39 % (at 2h) in cortex and 36 % (at 3.5h) in corpus callosum of the initial value. After the decrease, rADC starts to increase and normalizes around 2 weeks in subcortex, 1 week in cortex and 1-2 days in corpus callosum. Afterwards rADC increases in all tissues (figure 24). In cortex and subcortex, rADC increases steadily after the normalization, up to 4-6 weeks. In corpus callosum, where rADC normalizes substantially earlier compared to the other tissues, rADC reaches the maximum already at a third day and decreases afterwards. In table 4, it was tested whether there is a difference in rADC between the tissues at each time point.

rFA of subcortical regions is significantly different from the normal over the time period from 1 to 4 days ($p < 0.01$) (figure 24 (a)). In the cortical regions, rFA is significantly different from the normal at the time point 1w ($p < 0.04$) (figure 24 (b). In the corpus callosum regions, rFA is significantly different from the normal at the time points 2d, 3d, and 4d ($p < 0.02$) (figure 24 (c)). After the MCAO, rFA-value of cortical regions decreases 42 % (up to 3 days), subcortical decreases 55 % (up to 1 day), and corpus callosum decreases 50 % (up to 4 days) of the initial value. In table 4, it was tested whether there is a difference in rFA between the tissues at each time point.

Table 4. Table presents the t-test results. Tissue parameters (rADC and rFA) are compared at each time point during the 8 weeks observation period (2h, 3.5h, 1d, 2d, 3d, 4d, 1w, 2w, 4w, 6w, and 8w after MCAO). Significantly different time points are presented with their p-values.

TRANSIENT ISCHEMIA	
rADC	
cortex vs. subcortex	***1w (p = 0.013)***
corpus callosum vs. cortex	***2d (p = 0.01), 3d (p < 0.001), 4d (p < 0.001), 1w (p < 0.016)***
corpus callosum vs. subcortex	***2d (p < 0.001), 3d (p < 0.001), 4d (p = 0.001), 1w (p < 0.001), 6w (p = 0.046)***
rFA	
cortex vs. subcortex	***3.5h (p = 0.014), 1d (p = 0.004)***
corpus callosum vs. cortex	***6w (p = 0.027)***
corpus callosum vs. subcortex	***1d (p = 0.006), 2w (p = 0.043)***

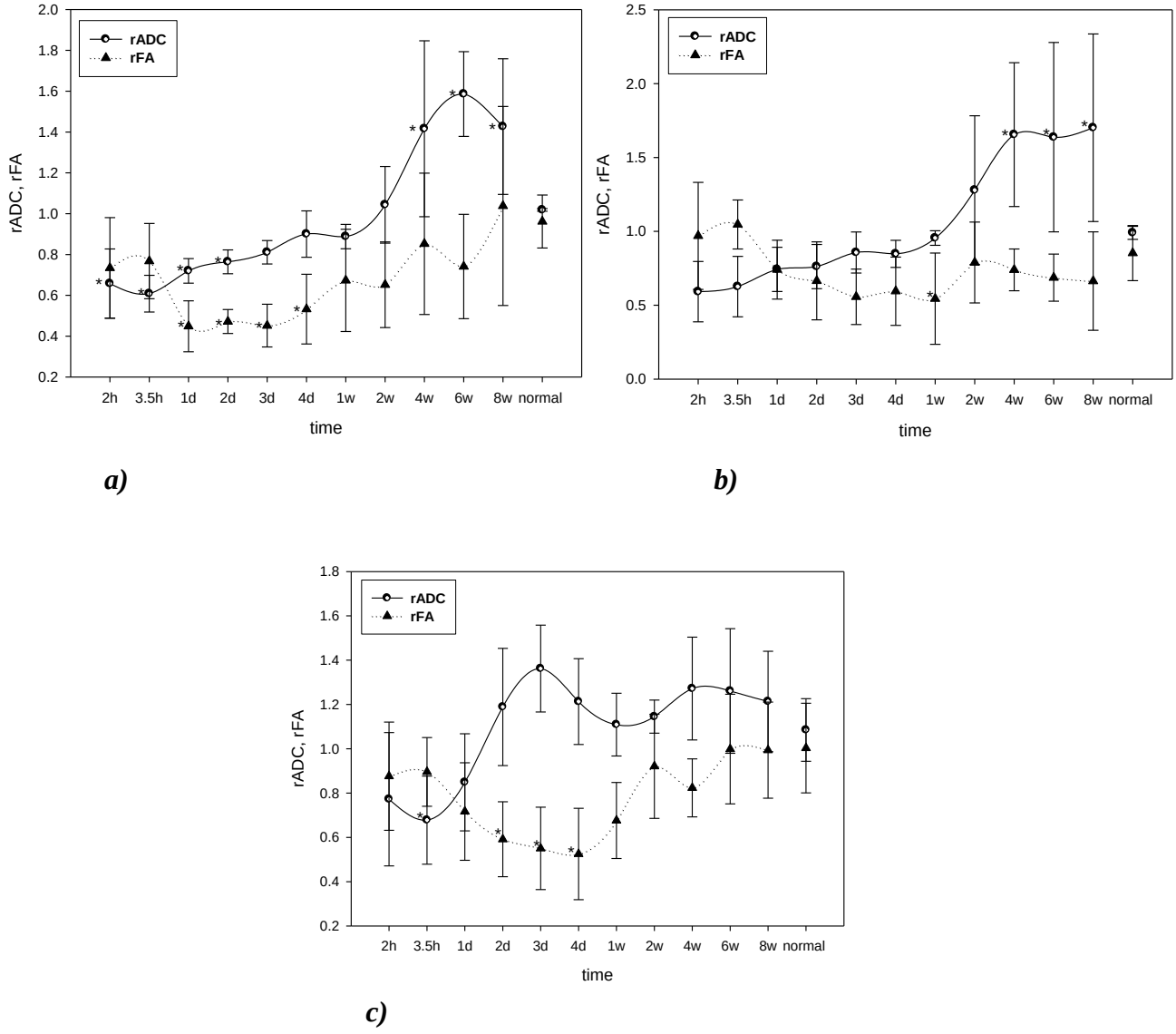

24) a) (subcortex), b) (cortex), and c) (corpus callosum): Each point is a ratio between ischemic tissue and their contralateral position. The evolution of DTI indices, rFA and rADC, over 8 weeks (2 hours – 8 weeks), is presented for subcortex, cortex, and corpus callosum. Normal presents the ratio between healthy right and left hemisphere in healthy animals. Time points that are significantly different from the normal are marked with an asterisk (*). In the a) (subcortex) (*) stands at 2h, 3.5h, 1d, 2d, 4w 6w, 8w (rADC) and 1d, 2d, 3d, 4d (rFA). In the b) (cortex) (*) stands at 4w, 6w, 8w (rADC) and 1w (rFA). (*). In the c) (corpus callosum) (*) stands at 3.5h (rADC) and 2d, 3d, 4d (rFA).

9.3.2 Ratio of T2 and T1

The absolute values of T2 and T1 from ischemic and contralateral side are presented in appendix B (Table B2). The absolute values of T2 and T1 in normal appearing hemisphere are not significantly different from healthy animals in throughout the observation period (2 hours – 8 weeks) ($p > 0.05$).

rT2 is significantly different from the normal in the time points 4w, 6w (cortex, $p < 0.02$), 1d, 2d, 3d, 4d, 4w, 6w (subcortex, $p < 0.01$), and 1d, 2d, 3d, 4d (corpus callosum, $p < 0.01$) (figure 25 (a)). 2 hours after MCAO, rT2 in all the tissues increases and reaches the first maximum on 1-2 days. In cortex and subcortex, the first maximum is followed by the second peak at 4 weeks. Meanwhile, rT2 of corpus callosum is decreasing to the level of the normal. When cortical and subcortical regions start to reach to the second peak, rT2 of cortical region clearly increases more than in the subcortical regions. In table 5, it was tested whether there is a difference in rT2 between the tissues at each time point.

rT1 is significantly different from the normal at 4w, 6w, 8w (cortex, $p < 0.01$), 1d, 2d, 4w, 6w (subcortex, $p < 0.01$), and corpus callosum is not significantly different from the normal at any time point (figure 25 (b)). 2 hours after MCAO, rT1 of cortical and subcortical regions is higher than the normal, and increases afterwards. In cortical regions, rT1 starts to increase more rapidly after 2 weeks, and stays high over the time period from 4 to 8 weeks. Subcortical regions are significantly different from the normal already at the first day (but decrease afterwards), and later over the time period from 4 to 6 weeks. At 8-weeks time point, subcortical regions normalize while cortical regions still remain high. In table 5, it was tested whether there is a difference in rT1 between the tissues at each time point.

Table 5. Table presents the t-test results. Tissue parameters (rT2 and rT1) are compared at each time point during the 8 weeks observation period (2h, 3.5h, 1d, 2d, 3d, 4d, 1w, 2w, 4w, 6w, and 8w after MCAO). Significantly different time points are presented with their p-values.

TRANSIENT ISCHEMIA	
rT2	
cortex vs. subcortex	***4w (p < 0.05), 8w (p < 0.03)***
corpus callosum vs. cortex	***2w (p = 0.014), 4w (p < 0.001), 6w (p = 0.021), 8w (p = 0.012)***
corpus callosum vs. subcortex	***2w (p < 0.001), 4w (p = 0.008), 6w (p = 0.023), 8w (p = 0.010)***
rT1	
cortex vs. subcortex	***in all the time points p > 0.05***
corpus callosum vs. cortex	***3d (p = 0.046), 4w (p = 0.02), 6w (p = 0.039), 8w (p = 0.012)***
corpus callosum vs. subcortex	***2w (p = 0.044), 4w (p = 0.039)***

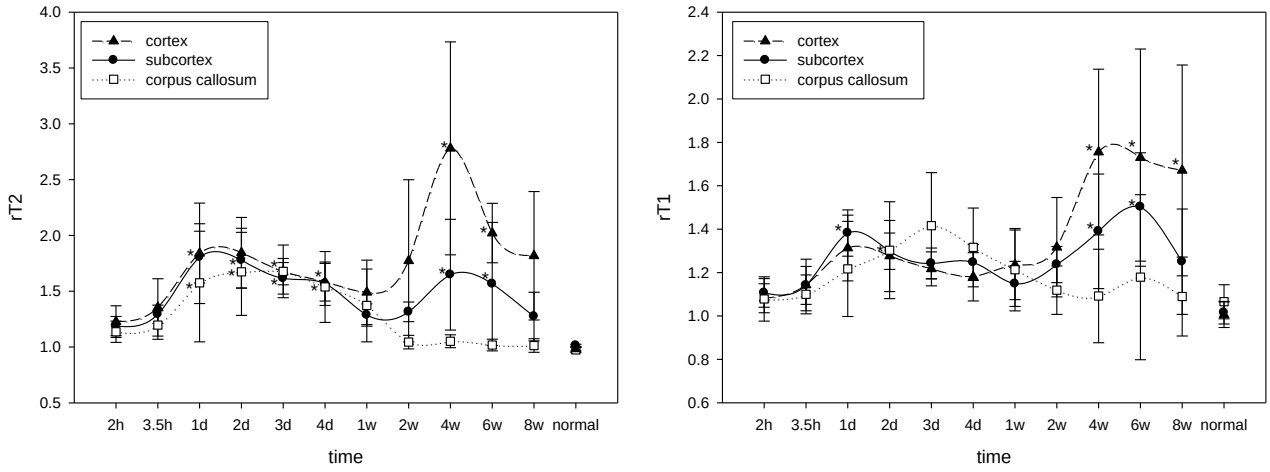

a) ***b)***

25) a) (rT2) and b) (rT1): Each point is a ratio of ischemic tissue and their contralateral position. The evolution of rT2 and rT1, over 8 weeks (2 hours – 8 weeks), after transient MCAO, is presented for subcortical, cortical, and corpus callosum regions. Normal presents the ratio between healthy right and left hemisphere in healthy animals. Time points that are significantly different from the normal are marked with an asterisk (*). In the a) (rT2) (*) stands at 4w, 6w (cortex), 1d, 2d, 3d, 4d, 4w, 6w (subcortex) and 1d, 2d, 3d, 4d (corpus callosum). In the b) (rT1) (*) stands at 4w, 6w, 8w (cortex), 1d, 2d, 4w, 6w (subcortex).

9.4 Difference between permanent and transient MCAO

9.4.1 Ratio of ADC and FA

Figures 26, 27, and 28 present rADC- and rFA- evolution after permanent and transient ischemia in subcortical-, cortical-, and in corpus callosum regions. In table 6, it was tested whether there is a difference in permanent and transient groups in each tissue (cortex, subcortex, and corpus callosum), at each time point (2h, 3.5h, 1d, 2d, 3d, 4d, 1w, 2w, 4w, 6w, and 8w).

9.4.1.1 Regions in the cortex

In table 6, while comparing transient and permanent ischemia groups in cortical regions, there is no difference in rADC at any time point during the 8 weeks observation period. rADC values in both groups increase steadily until the fourth day after MCAO (figure 26 (a)). After the fourth day, rADC of transient group continues increasing, but more rapidly than the permanent rADC does.

In table 6, while comparing transient and permanent group in cortical regions, there is no difference in rFA at any time point during the 8 weeks observation period. In figure 26 (b), rFA stays stable in both groups after the first day.

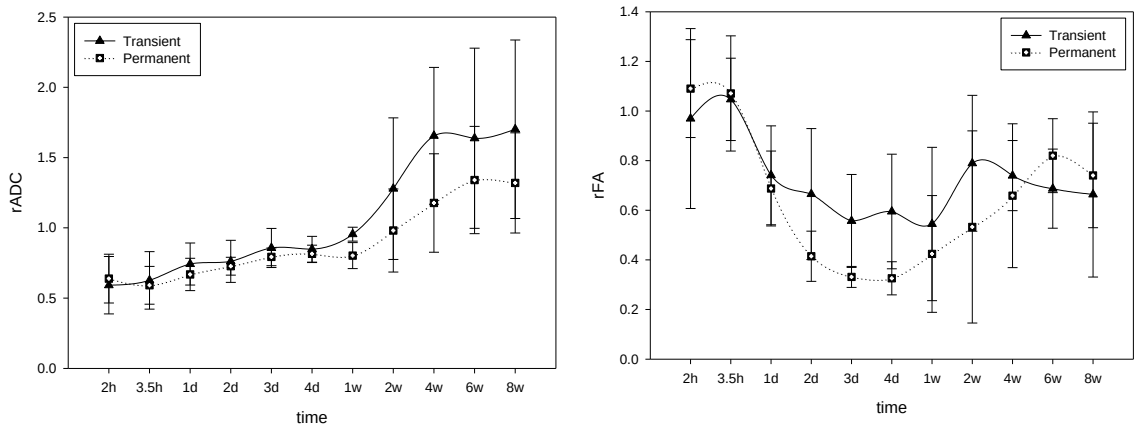

a) ***b)***

26) The evolution of rADC (a) and rFA (b) in cortical regions over 8 weeks (2 hours – 8 weeks) after permanent and transient ischemia.

9.4.1.2 Regions in the subcortex

In table 6, while comparing transient and permanent ischemia groups in subcortical regions, there is a significant difference in rADC at time points 3.5h, 3d, 4d, 1w, 2w, 4w, and 6w. As seen in the figure 27 (a), rADC evolves in a similar way until the second day in transient and permanent groups while it increases steadily. After that, rADC of the transient group continues increasing and contradictorily, rADC of permanent ischemia group starts to reduce. This reduction in permanent group is followed by an increase later in 1 week that continues up to 8 weeks. At 8-week time point, rADC of transient and permanent ischemia group reach the same high value.

In table 6, while comparing transient and permanent ischemia group in cortical regions, there was found no significant difference in rFA at any time point during the 8 weeks observation period. As seen in the figure 27 (b), rFA evolves similarly until 1 week. After that, rFA of the transient ischemia group continues increasing, and contrary to that, rFA of the permanent group decreases suddenly at 2-week time point, but afterwards returns to the level of transient ischemia group.

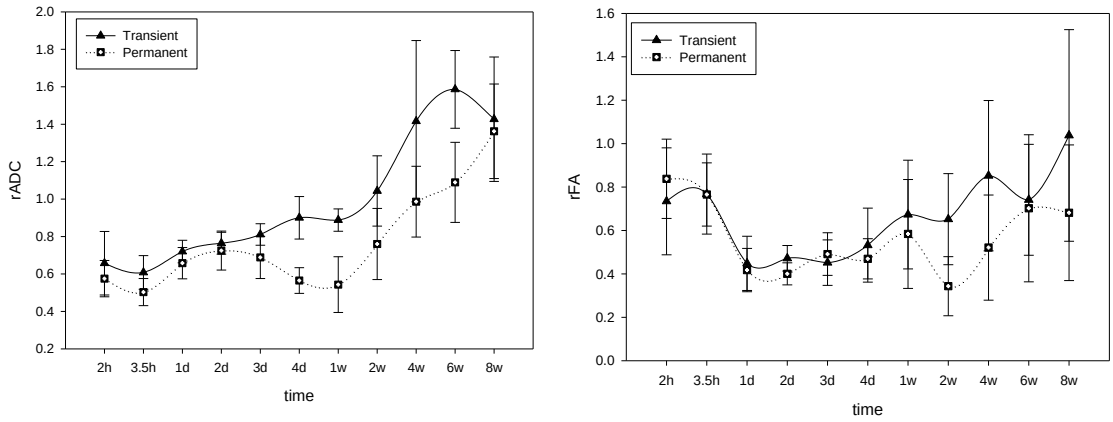

a) ***b)***

27) The evolution of rADC (a) and rFA (b) in subcortical regions over 8 weeks (2 hours – 8 weeks) after permanent and transient ischemia.

9.4.1.3 Regions in the corpus callosum

Comparison of transient and permanent ischemia groups in corpus callosum regions, show a significant difference in rADC at time points 2h, 1d, 2d, 3d, 4d, and 1w (Table 6). In the transient ischemia group, rADC increases strongly after 3.5 hours, whereas rADC decreases in the permanent ischemia group (figure 28 (a)). Afterwards, rADC of permanent ischemia group pseudonormalized 1 week later than the group of transient. Despite the inverse behavior of rADC over the time period from 3.5 hours to 4 weeks, starting at 6 weeks and later, rADC of transient and permanent ischemia groups was fairly similar.

In table 6, while comparing transient and permanent ischemia groups in corpus callosum regions, there is a significant difference in rFA at time points 3d and 4d. In figure 28 (b), rFA of permanent and transient ischemia groups' stays stable after day 1.

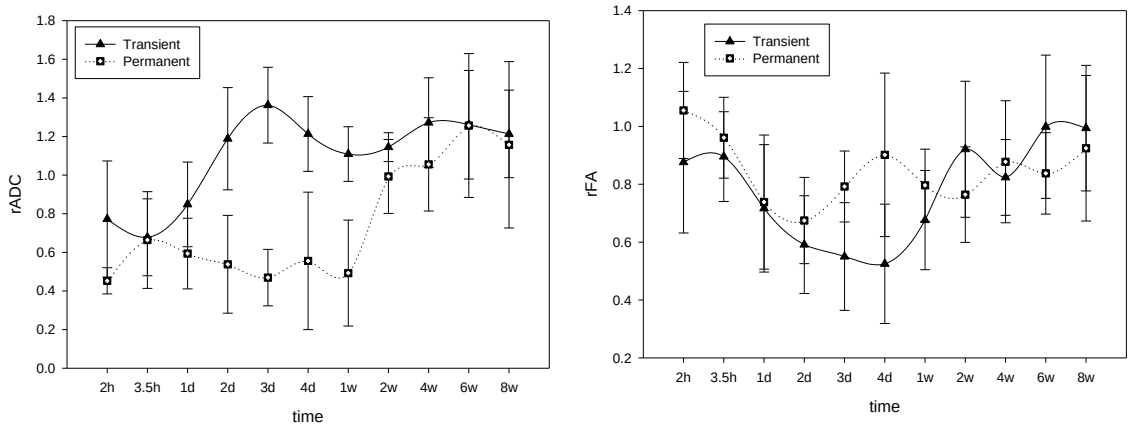

28) The evolution of rADC (a) and rFA (b) in corpus callosum regions over 8 weeks (2 hours – 8 weeks) after permanent and transient ischemia.

Table 6. Table presents the t-test results. Tissues are compared at each time point (2h, 3.5h, 1d, 2d, 3d, 4d, 1w, 2w, 4w, 6w, and 8w after MCAO) and over time for 8 weeks. The difference is significant when p-value is < 0.05. Significantly different time points are presented with their p-values.

PERMANENT VS. TRANSIENT ISCHEMIA	
rADC	
cortex	***all time points p > 0.05***
subcortex	***3.5h (p =0.027), 3d (p = 0.011), 4d (p < 0.001), 1w (p < 0.001), 2w (p = 0.04), 6w (p = 0.006)***
corpus callosum	***2h (p = 0.01), 1d (p = 0.016), 2d (p < 0.001), 3d (p < 0.001), 4d (p < 0.001), 1w (p < 0.001)***
rFA	
cortex	***all time points p > 0.05***
subcortex	***all time points p > 0.05***
corpus callosum	***3d (p = 0.01), 4d (p = 0.009)***

9.4.2 Ratio of T1 and T2

Figures 29, 30, and 31 present rT2- and rT1- evolution after permanent and transient ischemia in subcortical-, cortical-, and in corpus callosum regions. In table 7, it was tested whether there is a difference in permanent and transient ischemia groups in each tissue (cortex, subcortex, and corpus callosum), at each time point (2h, 3.5h, 1d, 2d, 3d, 4d, 1w, 2w, 4w, 6w, and 8w).

9.4.2.1 Regions in the cortex

In table 7, while comparing transient and permanent ischemia groups in cortical regions, there is a significant difference in rT2 at time points 2h and 3.5h. Both groups evolve similarly over the observation period (29 (a)). Only difference occurs at 4-week time point where rT2 reaches the second peak in transient group that is higher compared to permanent group (but not significantly).

In table 7, while comparing transient and permanent group in cortical regions, there is no significant difference in rT1, between the times points, during the 8 weeks observation period. In figure 29 (b), rT1 increases steadily up to 8 weeks in both tissues.

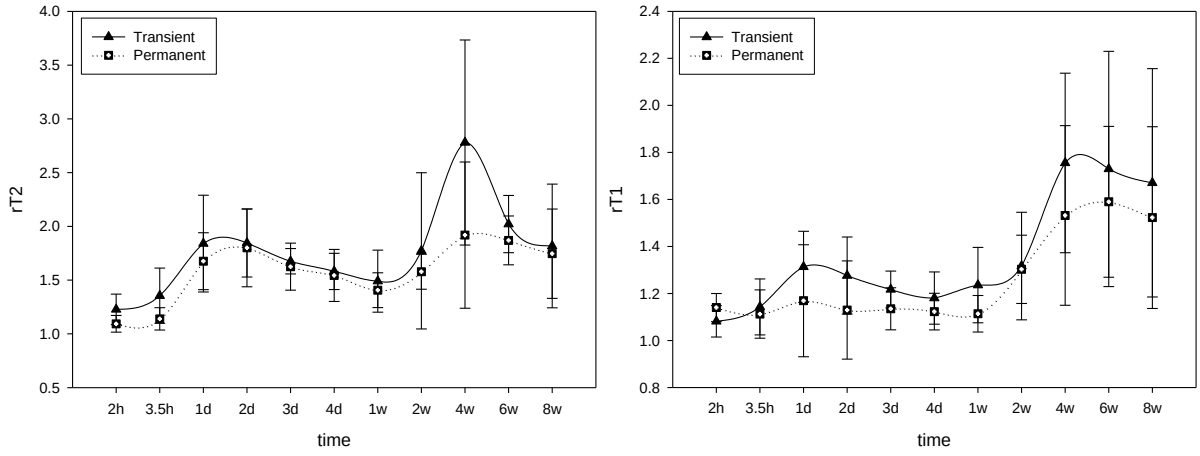

a) ***b)***

29) The evolution of rT2 (a) and rT1 (b) in cortex regions over 8 weeks (2 hours – 8 weeks) after permanent and transient ischemia.

9.4.2.2 Regions in the subcortex

In table 7, while comparing transient and permanent ischemia groups in subcortical regions, there is a significant difference in rT2 at time points 1w and 2w. Both groups evolve fairly similarly over the observation period (figure 30 (a)).

In table 7, while comparing transient and permanent group in subcortical regions, there is a significant difference in rT1 at time points 1d, 1w, and 2w. In figure 30 (b), transient and permanent ischemia seem to evolve fairly similarly up to the fourth day. After the fourth day, increasing of rT1 is more pronounced in the permanent ischemia group than in the transient ischemia group. At 8-week time point, permanent ischemia group seems to increase again, while transient ischemia group decreases.

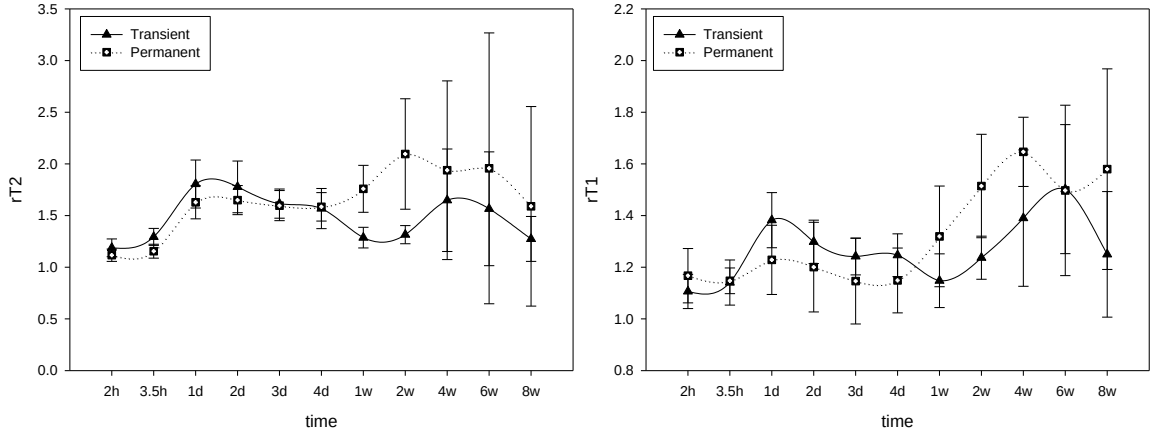

30) The evolution of rT2 (left) and rT1 (right) in subcortical regions over 8 weeks (2 hours – 8 weeks) after permanent and transient ischemia

9.4.2.3 Regions in the corpus callosum

In table 7, while comparing transient and permanent ischemia groups in corpus callosum regions, there is a significant difference in rT2 at time points 2h and 1d. In figure 31 (a), after rT2 increases in transient ischemia group, it remains high over several days and decreases afterwards. Meanwhile, rT2 of permanent ischemia group increases more strongly and reaches the maximum value in one time point and decreases afterwards.

In table 7, while comparing rT1 of transient and permanent ischemia group in corpus callosum regions, there is no significant difference in any time point, during the 8 weeks observation period. In figure 31 (b), rT1 evolves in a similar way after transient and permanent ischemia.

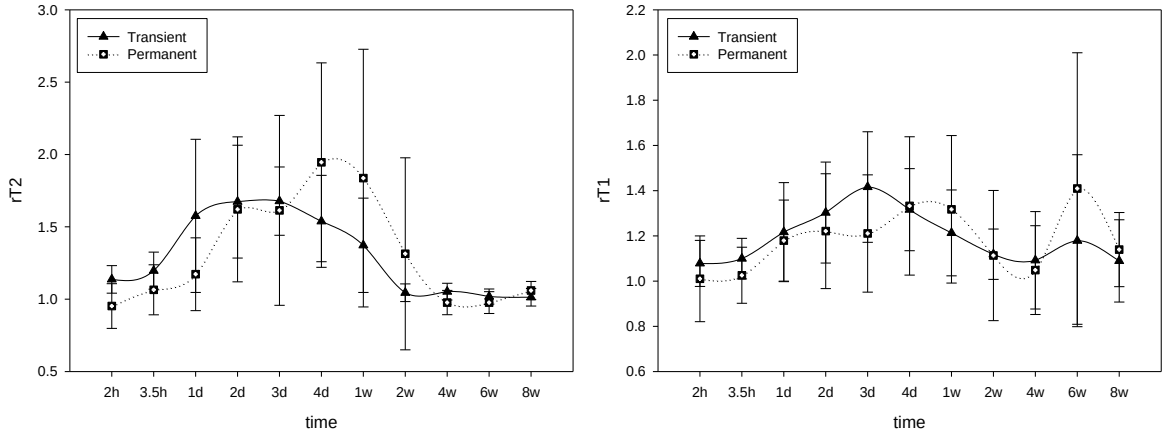

a) ***b)***

31) The evolution of rT2 (left) and rT1 (right) in corpus callosum regions over 8 weeks (2 hours – 8 weeks) after permanent and transient ischemia

Table 7. Table presents the t-test results. Tissues are compared at each time point (2h, 3.5h, 1d, 2d, 3d, 4d, 1w, 2w, 4w, 6w, and 8w after MCAO) and over time for 8 weeks. Significantly different time points are presented with their p-values.

PERMANENT VS. TRANSIENT ISCHEMIA	
rT2	
cortex	***2h (p = 0.024), 3.5h (p = 0.026)***
subcortex	***3.5h (0.002), 1w (p < 0.001). 2w (p = 0.002)***
corpus callosum	***2h (p = 0.008), 1d (p = 0.046)***
rT1	
cortex	***all time points p > 0.05***
subcortex	***1d (p = 0.019), 1w (p = 0.039), 2w (p = 0.009)***
corpus callosum	***all time points p > 0.05***

9.5 Lesion volumes

Lesion volumes are measured from multislice (n = 7) EPI. Seven slices with a slice thickness of 2 mm encompassed the whole brain.

I compare the lesion volumes after transient and permanent ischemia and the results are presented in figure 32. The lesion volume is larger at several times in the permanent ischemia group where they reach the statistical significance at time points (2h ($p = 0.038$), 3.5h ($p = 0.008$), 1d ($p = 0.006$), 4d ($p = 0.042$), 1w ($p = 0.006$), 2w ($p = 0.017$), 4w ($p = 0.005$), 6w ($p = 0.002$), and 8w ($p = 0.006$)).

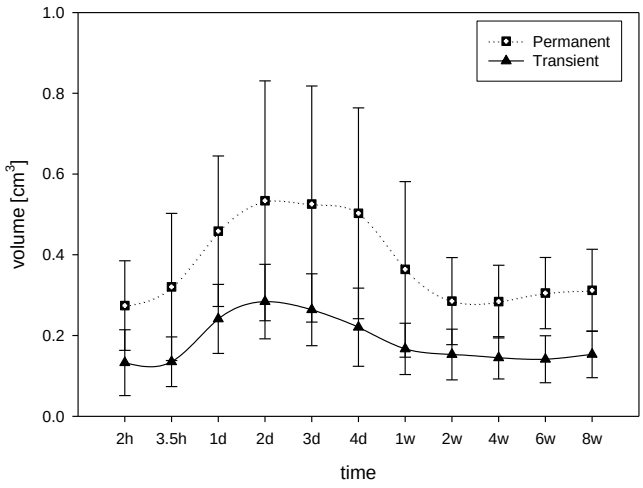

32) The evolution of lesion volume over 8 weeks (2 hours - 8 weeks) after permanent and transient ischemia.

10 DISCUSSION

10.1 Preparation of the DTI and the imaging

The work started by optimization of the DTI acquisition protocol. While taking into consideration the requirements that the clinical imaging sets (limited imaging time, thin slice thickness, SNR etc.), 30 NDGDs and averaging (NA = 2) was used in this study. Skare et al (Skare et al., 2000) earlier proved that by using 30 NDGDs provides better measures of DTI than the conventional 6 NDGDs, and it is recommended that one should use as many NDGDs as the imaging time allows (Jones et al., 1999). Simulation-based studies have been utilized to optimize DTI acquisition and report that increasing the directional resolution of DTI dataset (NDGD) is preferable to repeating observations (NA) if the imaging time is equal (Landman 2007). The parameters (NDGD = 30 and NA = 2) for this study was also supported by another work where they used the same parameters (Jones et al., 1999).

The optimum *b*-value for the DTI was obtained by using a simple rule of thumb: optimal *b*-value multiplied by the ADC of the tissue under investigation should be close to 1 (Mukherjee et al., 2008b). While the ADC for brain tissue ranges from 0.66×10^{-3} mm^2/sec to 0.86×10^{-3} mm^2/sec, depending on the amount of GM and WM, it had to be compromised between those. I chose *b*-value to be $b = 1500$ s/mm^2.

Previously it has been demonstrated how important it is to pay attention on SNR when working with DTI (Pierpaoli and Basser, 1996, Bastin et al., 1998, Papadakis et al., 2000, Anderson, 2001, Jones, 2004). By doing testing imaging with a healthy rat, with SNR_0 (SNR for $b = 0$ s/mm^2 image) ranging from 20 to 50, I found that when $SNR_0 \sim 22$, mean diffusivity of the diffusion tensor became stable. With fractional anisotropy, SNR had to be slightly larger to gain a balanced value ($SNR_0 \sim 30$). While the ROIs were placed to cortex, subcortex and corpus callosum, it could be noticed that all the tissues balanced about simultaneously. According to these test results, I chose SNR_0 to be 40. By preparing a water phantom, I sought for reference value of isotropic diffusion. This way I can find out how good estimation of the isotropic and anisotropic diffusion does the system give. In theory, the water phantom should yield a FA value of zero. But, in practice, because of the noise and phase fluctuation, the value of water is a nonzero-value (Madi et al., 2005). The result from the isotropic water phantom, with chosen SNR_0 ($SNR_0 = 40$), was fairly similar with the earlier published data from an isotropic environment (Madi et al., 2005). In addition, repeated measurement with the water phantom demonstrated good reproducibility.

To minimize motion artifacts during imaging, animals were under anesthesia and the head was fixed in a holder with tooth and ear bars to avoid most of the movement during the imaging. Still, there exists a venous pulsation of the brain that might have caused some artifact. The artifact from the venous pulsation could be removed nearly entirely by using a cardiac triggering (Dietrich et al., 2000, Summers et al., 2006). The flipside of the triggering is that it increases the imaging time two to three times

(Lewis et al., 1986). I did not have an opportunity to use triggering. Still, some study find the use of cardiac triggering not necessary anymore while nowadays systems offer higher spatial resolution and different pre- and post-reconstructions are done to the image (Robson and Porter, 2005). Addition to the results of Robson et all (Robson and Porter, 2005), all the recent brain DTI studies that I am referring to in this present work, worked without triggering. This way, the present results can also be considered trustworthy.

10.2 ADC and FA of control animals

The results of ADC measurements in cortex, subcortex and corpus callosum are fairly similar with the previous works that are listed in table 1. Also the value of FA fits in to the range of the previous publications (table 1).

In table 1, some of the works that I am referring to, used only 6 - 12 NDGSs, while in the present study 30 NDGDs were used. Smaller number of NDGDs would result in a lower SNR as discussed earlier in chapter 5. ADC is not as sensitive to SNR as FA; it is also seen in table 1 where results of ADC are fairly similar among all the studies (NDGD varies from 6 to 32) and results of FA can have fairly large variations among studies.

Among the eight healthy animals that were studied, SD of FA was fairly large inside all the tissues (cortex, subcortex and corpus callosum). The result with a larger SD, in the corpus callosum, was expected because similar findings with corpus callosum have been published before in human brain (Chepuri et al., 2002). It has been explained by regional differences of the microscopic structure of the corpus callosum, as it can be divided into several sections, all having distinct characteristic features (factors that can vary inside corpus callosum 1) tighter packing of axons, 2) less permeable myelin sheats, 3) fewer obliquely oriented axons, 4) altered radius of individual axons, and 5) the presence of structures other than myelin sheaths within the corpus callosum that restrict water diffusion (Chepuri et al., 2002, Hasan et al., 2005). In addition to corpus callosum, these features are present in the subcortex, but makes only small contribution to WM. This is because the volume of the WM is not uniform between different regions of the subcortex. Hence, dislocation of a ROI by only few millimeters may result in significant changes in anisotropy values and may introduce a fairly large variation between the animals. Other reasons that can increase the SD are the partial volume effects and possible movement artifacts (Chapter 10.1). Because of the fairly low resolution (MTX = 128 x 128) of EPI, intravoxel partial voluming can influence on the observed diffusion and anisotropy measures (Pfefferbaum and Sullivan, 2003). It means that possible ‘unwanted’ including (because of the fairly low resolution) of GM and/or CSF in the WM ROI will result as an inaccurate estimation of ADC and FA.

10.3 FA, ADC, T1, and T2 after transient and permanent ischemia in cortex, subcortex, and corpus callosum

10.3.1 Anisotropy of the brain tissues after permanent ischemia

In this present work, rFA decreased after permanent MCAO and became significantly different from the normal. In subcortex, rFA was significantly different from the normal over time period from 1 day to 4 weeks, in cortical regions from 2 days to 1 week, and in corpus callosum only at one time point at 2 days. The overall behavior of rFA in the corpus callosum could be described to be 'oscillatory' throughout the 8 weeks observation period. Decreasing of FA in the ischemic tissue has been observed in the earlier studies and it has been reported to last up to 90 days in humans (Munoz Maniega et al., 2004) and 30 days in macaques (Liu et al., 2007). To my knowledge the evolution of FA after permanent MCAO in rats has not been previously reported. This reduction of the rFA characterizes the loss of structural integrity in the injured tissue and is consistent with the progression of ischemic changes. It was noticed that after permanent ischemia, rFA of cortical and subcortical regions decreased more and under longer period of time than rFA of the corpus callosum regions.

There is a different contribution of WM and GM in subcortical regions (14 % WM and 86 % GM), cortical regions are a GM-dominant, and corpus callosum is formed of WM. While WM and GM have differences in cellular constituents; the cerebral blood flow and metabolism are also characteristic for the tissue and it results in different vulnerability to ischemia and as a different outcome (Arakawa et al., 2006). As I found more pronounced decrease of diffusion anisotropy in GM, I might agree with the previous studies about the more vulnerable GM. It has been proved in animal (Marcoux et al., 1982) and in human (Falcao et al., 2004, Arakawa et al., 2006) studies that GM is more vulnerable than WM to ischemia. In WM, there are no neuronal cell bodies, dendrites, or synapses and this is likely the reason why it is thought to be less injured after ischemia. Despite the common belief of ischemia resistant WM, it has been shown that a severe damage to nerve fibers occurs after the ischemia both in patients (Bristow et al., 2005) and in rats with permanent ischemia (Pantoni et al., 1996).

After being significantly different from the normal, rFA of the brain tissues (cortex, subcortex, and corpus callosum) normalized. Increased organization of the extracellular space and movement of water into the more restricted environment of the intracellular space may both occur with cytotoxic edema, and both of these models result as an increased FA (Green et al., 2002). Zelaya et al (Zelaya et al., 1999) also reported increasing of FA in the chronic phase (> 90 days) but not yet normalization, and they explained the increasing by the development of glial scar tissue. Whereas Liu et al (Liu et al., 2007) reported continuous decreasing of rFA until 35 days after permanent ischemia in macaques, which is though to arise from the progressive loss of the tissues' structural integrity. There are no such studies that would have systematically followed the evolution of DTI parameters after ischemia over such long period as I did. This might be one the reasons why there are no

published data about the normalization of FA in the chronic phase, and this makes the present study novel. In the present work, meanwhile FA normalize, T1 and T2 do not normalize (Chapter 9.2.2), which refers to the presence of some kind of abnormality in the tissue.

When comparing the absolute values of FA (Table A1, appendix A) over the time period from 2 hours to 8 weeks, it was found that corpus callosum and subcortex are significantly different from the cortex ($p < 0.05$), in all the time points. Maniega et al (Munoz Maniega et al., 2004) reported similar results 3 month after ischemia when they compared FA of WM and GM in stroke patients. This observation supports the idea that after permanent ischemia, WM regions still contain organized axonal structure and FA of corpus callosum and subcortical regions does not decrease to the level of isotropic tissues.

10.3.2 Diffusivity of the brain tissues after permanent ischemia

The results of rADC followed the trend of previous works: it is well established that acute brain ischemia causes a decrease in rADC that is followed by renormalization (pseudonormalization) and later increasing both in rats (Hoehn-Berlage et al., 1995, Rudin et al., 2001, Doerfler et al., 2002) and in patients (Marks et al., 1996, Schlaug et al., 1997, Yang et al., 1999, Zelaya et al., 1999). Because patients in these former studies have not received tPA medication medication (that is given to the stroke patients to inhibit the organization of the blood cloth), I call them "human nonreperfusion" – studies (Liu et al., 2007) and refer to them as permanent ischemia.

After permanent ischemia, in the first time point (2 hours after MCAO), rADC was significantly different from the normal in all the tissues; while rADC decrease 39 % in cortical-, 51 % in subcortical- and 58 % in corpus callosum regions. Previously it has been reported 33 to 74 % decrease in rats (Benveniste et al., 1992, Hoehn-Berlage et al., 1995) and 17 to 59 % decrease in patients (Marks et al., 1996, Schlaug et al., 1997, Yang et al., 1999). In the present work, after rADC reduced, it remained depressed until 1 day in cortical regions and until 1 week in subcortical and corpus callosum regions, after permanent ischemia. In previous rat studies, ADC remained reduced for 2 to 4 days (Rudin et al., 2001) and for 4 to 10 days in patients (Marks et al., 1996, Schlaug et al., 1997), after ischemia.

Decreasing of rADC after MCAO, which can be found in all the tissues, is known to be a consequence from the development of vasogenic edema when the loss of cell membrane integrity grows (Helpern et al., 1993, Knight et al., 1994, Jiang et al., 1997, Munoz Maniega et al., 2004). It has been speculated, both in animal and patient studies, that a strong decrease of ADC is associated with greater risk of irreversibility of the lesion (Hasegawa et al., 1994, Durukan and Tatlisumak, 2009). Also, Schlaug et al (Schlaug et al., 1997) suggest in a patient study that the pronounced reduction of rADC may reflect ongoing or progressive cytotoxic edema to a greater degree than extracellular edema and cell death. Fiehler and colleagues (Warach et al., 1995, Fiehler et al., 2002) reported that severe ADC drop does not predict tissue viability while severe ADC decrease may completely recover. However, normalization of ADC does not necessarily reflect total salvage of brain tissue after the ischemia (Li et al., 2000a, Neumann-Haefelin et al., 2000). Together

with T2-weighted images, the actual ADC changes can help to identify between tissues that has a potential to recover, that is in progression to necrosis, or that is already irreversibly damaged (Welch et al., 1995, van Dorsten et al., 2002).

In this study, rADC pseudonormalized 2 days-4 weeks (24 to 600 hours) after permanent ischemia and the general trend of rADC evolution (over the 8 weeks observation period) was similar in all tissues. However, different tissues pseudonormalized in different time points: cortical regions at 2 days, subcortical regions at 4 weeks and corpus callosum regions at 2 weeks after permanent MCAO. It is known that pseudonormalization of ADC after stroke varies much between patient and animal model; in humans it takes place around 230 hours after the onset (Marks et al., 1996, Schlaug et al., 1997, Yang et al., 1999, Zelaya et al., 1999), in rats 72 to 168 hours after MCAO (Knight et al., 1994, Doerfler et al., 2002), and in macaques 200 to 300 hours after MCAO (Liu et al., 2007). According to literature, ADC changes after stroke in rats seem to be more rapid than with patients. In the present study, the time of pseudonormalization varies much from 48 to 670 hours. This relatively large difference arises from the different tissues.

10.3.3 T2 and T1 of the brain tissues after permanent ischemia

Addition to rFA and rADC, I investigated the evolution of the ischemia with rT1 and rT2. Numerous works have reported similar evolution of T1 and T2 after permanent ischemia as I did (Ishii et al., 1998, Kettunen et al., 2000, Li et al., 2000a, Makela et al., 2002, van Dorsten et al., 2002). After the MCAO in cortical and subcortical regions, rT1 and rT2 increase gradually until they reach the maximum value, and stay high afterwards. Corpus callosum makes an exception while after the maximum value; it decreases to the level of normal and remains there.

There is a difference in the timing of the evolution between human and animal; maximum value of T2 in the infarcted tissue occurs approximately after 140 hours in humans (Marks et al., 1996, Lansberg et al., 2001), 24 to 48 hours in rats (Knight et al., 1994, Li et al., 2000a, Neumann-Haefelin et al., 2000, Sotak, 2002), 72 hours in macaques (Liu et al., 2007) and 24 to 96 hours in our work (the first peak value after MCAO). However, T2 elevation after ischemia, between animal model and in patient is known to be more comparable than the evolution of ADC after the stroke (ADC pseudonormalizes much later in human than in rat) (Liu et al., 2007).

1 week after MCAO, cortical and subcortical regions increased strongly and became significantly different from the normal, while corpus callosum regions decreased to the level of normal and maintained there.

It is generally considered that increasing of T2 and T1 are associated with vasogenic edema and irreversible ischemia when such changes occur several hours after stroke event (Kato et al., 1986, Naruse et al., 1991). Following the ischemia, water is thought to gather in the brain once the BBB is disrupted and the increase in overall water content is believed to account for the extended T1 and T2 observed several hours after ischemia (Kato et al., 1986, Mintorovitch et al., 1991, Naruse et al., 1991). Some studies have reported early moments, minutes or even seconds, changes in T1 and T2 with high field (4.7-9.4T) system studies (Ewing et al., 1999, Kettunen

et al., 2000, Lythgoe et al., 2000). These acute changes are known to result from the cessation of blood flow in the rat brain (Detre et al., 1992), and at the moment it is under investigation whether these changes are related to the MCAO-model (Lythgoe et al., 2000). However, over a long time scale after MCAO, like in the present work, these acute changes are very minor compared to the overall evolution of T1 and T2. Also, in the present work, the animals were not scanned minutes after MCAO.

10.3.4 Anisotropy of the brain tissues after transient ischemia

In the present work, rFA decreased after transient MCAO and became significantly different from the normal. rFA was significantly different from the normal over the time period of 1 to 4 days in subcortex and 2 to 4 days in corpus callosum. Compared to the cortical regions, the rFA-decrease in subcortical and corpus callosum regions was more rapid and it lasted over longer period of time; cortical regions were significantly different from the normal only in one time point and the trend was 'oscillatory' during the whole 8 weeks observation period. Decreasing of FA in the ischemic tissue has been observed in the earlier studies and it has been reported to last up to 90 days in rats (Carano et al., 2000), 5 to 90 days in humans (Zelaya et al., 1999) and 6 hours in macaques (Liu et al., 2007). Maniega et al and Yang et al (human nonreperfusion) (Yang et al., 1999, Munoz Maniega et al., 2004) also reported that FA of WM tissue decreased more rapidly than FA of GM tissue after the stroke onset in patients. In contrary, Carano et al (Carano et al., 2000) reported stronger decrease of rFA in cortex than in subcortex, after transient ischemia in rats. As it was mentioned earlier, the decreasing of FA is connected to the loss of tissue integrity. Now, when FA decreases more in WM, it might be thought that there is a bigger injury in the WM tissue. Commonly, GM has been considered to be more vulnerable because of its tissue content (neuronal cell bodies, dendrites and synapses). However, there are studies supporting the vulnerability of WM to ischemia (Pantoni et al., 1996, Bristow et al., 2005).

After the decrease of rFA, it had trend to normalize (1 to 2 weeks after MCAO) in all the tissues. Similarly to subcortex and corpus callosum, Liu et al (Liu et al., 2007) reported increasing of rFA but not normalization in a chronic phase after transient ischemia. These observations indicate the presence of organized axonal structure. It might be assumed that organized structures remain or recover in the chronic phase.

When comparing the absolute values of FA (Table B1, appendix B) over the time period from 2 hours to 8 weeks, it was found that corpus callosum and subcortex are significantly different from the cortex ($p < 0.05$), in all the time points. This observation supports the idea that even if FA of the corpus callosum and subcortical regions decreases the most as a percentage, these regions still contain organized axonal structure and do not decrease to the level of isotropic tissues.

10.3.5 Diffusivity of the brain tissues after transient ischemia

After transient MCAO, in cortical and subcortical region; rADC first decreased, which was followed by pseudonormalization and later increasing. According to the literature, similar observations are widely reported in rats (Jiang et al., 1993, Jiang et

al., 1997, Li et al., 2000a, Neumann-Haefelin et al., 2000) and in patients (Warach et al., 1995, Marks et al., 1999, Sorensen et al., 1999, Mukherjee et al., 2000).

After transient ischemia, in cortical and corpus callosum regions, the maximum reduction of rADC takes place at a time point 3.5 hours (rADC is significantly different compared to normal) where cortical regions decrease 39 % and corpus callosum 36 % from the initial value. In cortical region, rADC has the maximum decreasing at 2-hours time point (not significantly different from the normal), and it decreases 41 % from the initial value, but does not become significantly different from the normal. Previous works reported 30 to 70 % reduction in rat studies (Neumann-Haefelin et al., 2000, Sotak, 2002) and approximately 40 % reduction in human stroke (Warach et al., 1995, Mukherjee et al., 2000). After the maximum reduction of rADC, it starts to increase until normalization which is followed by an increase. In rat studies, ADC remains depressed for 1 to 7 days (Jiang et al., 1993, Knight et al., 1994, Neumann-Haefelin et al., 2000) and in patient studies for 4 to 10 days after ischemia (Warach et al., 1995, Marks et al., 1996, Schlaug et al., 1997, Mukherjee et al., 2000). Herein, I am comparing my work to patient studies hence they are mostly considered as transient ischemia (tPA treatment) (Durukan and Tatlisumak, 2009). In the literature, pseudonormalization of ADC varied much between the species; in humans with a mean around 50 to 100 hours (Knight et al., 1994, Marks et al., 1999), compared with 24 to 72 hours in rats (Li et al., 2000a, Neumann-Haefelin et al., 2000), 200 to 300 hours in macaques (Liu et al., 2007) and 72 hours in the present work. While rADC of cortical and subcortical regions pseudonormalize approximately at day 3 (72 hours), corpus callosum regions pseudonormalize already in a first day after transient MCAO. Marks et al (Marks et al., 1999) suggests that a pseudonormalization of ADC as early as 1 day after thrombolysis (tPA) represents reperfusion injury (after reperfusion the delivery of oxygen is “too fast” and the cells are unable to use all of it, and this leads to the formation of oxygen free radicals which are harmful (Chan, 1996) with early cell death. Phenomenon of early ADC rise is explained: 1) regions of vasogenic edema develop earlier in those cases that reperfuse more rapidly or 2) early reperfusion promotes more rapid cell death, which also alters the existing environment in which the water molecules exist (Marks et al., 1999). Both vasogenic edema and cell death have been shown to cause elevated ADC (Pierpaoli et al., 1993).

10.3.6 T2 and T1 of the brain tissues after transient ischemia

After ischemia, the evolution of rT1 and rT2 followed a well reported trend of these parameters (Ishii et al., 1998, Kettunen et al., 2000, Li et al., 2000a, Makela et al., 2002, van Dorsten et al., 2002). After the MCAO in cortical and subcortical regions, rT1 and rT2 increase gradually until they reach the maximum value. However, while rT1 and rT2 of cortical and subcortical regions increased, cortical regions increased substantially more compared to subcortical regions. In corpus callosum, after the maximum, rT2 and rT1 decreases to the level of normal and remains there.

1 week after transient ischemia, rT1 and rT2 enables to characterize all tissues with different contribution of WM and GM.

10.4 Comparing brain tissues after transient and permanent ischemia

As I discussed earlier in chapter 7, after ischemia, there is a progression of potentially reversible ischemic injury toward infarction. The transition from reversible to irreversible tissue injury is complicated and depends on the duration and the severity of ischemia (van Lookeren Campagne et al., 1999, Ginsberg, 2003). Also WM and GM have different vulnerability for ischemia (Arakawa et al., 2006). I am interested to find out whether DTI parameters and conventional T1 and T2 could reveal more about the tissue damage between transient and permanent ischemia and to find out whether there are differences between the tissues (cortex, subcortex, and corpus callosum).

While comparing groups of transient and permanent ischemia in cortical, subcortical, and corpus callosum regions; in cortical regions reperfusion did not have any impact on rADC or rFA. Meanwhile, in subcortical regions rADC was significantly different between the groups in time point 3.5h, over the time period from day 3 to 2 weeks, and at time point 6w, while rFA did not show a significant difference in any time point. In corpus callosum regions, rADC was significantly different between the groups at a time point 2h and over the time period from day 1 to 1 week. Meanwhile, rFA was significantly different at time points 3d and 4w. In overall, rFA seems to be less sensitive compared to ADC while it does not much differentiate between transient and permanent ischemia groups. However, I noticed that in the acute and subacute phase after permanent MCAO, rFA reduced more rapidly and under longer period of time in cortex and subcortex than in corpus callosum. Contradictory, after transient MCAO, rFA reduced more rapidly in corpus callosum than in cortex and subcortex. Finally the chronic phase, rFA normalized in all the tissues.

Both subcortical and corpus callosum regions have a contribution of WM and because of this, it might be assumed that some changes occur strictly in WM, which is causing the difference in ADC between the groups. Perhaps GM goes thought the major changes already in the early phase of ischemia and this way reperfusion after 90 minutes of ischemia does not have any impact on the evolution of DTI parameters. As it was mentioned earlier, several observations and my former speculation support the idea of GM with higher sensitivity to ischemia when compared to WM (Marcoux et al., 1982, Falcao et al., 2004, Arakawa et al., 2006).

Even if the difference between transient and permanent group is not always significant, ADC of all the tissues pseudonormalizes earlier after transient ischemia than after permanent ischemia. This result supports the earlier reported observation that the timecourse of ADC-changes in human reperfused stroke is accelerated compared with nonreperfused stroke (Liu et al., 2007).

Conventional parameters (rT1 and rT2) could not differentiate between transient and permanent ischemia; all the tissues showed only few points to be significantly different between the groups.

10.5 Evolution of lesion volume after permanent and transient ischemia

In the present study, 90 minutes reperfusion led to significantly smaller lesion volumes at most of the time points (2h, 3.5h, 1d, 4d, 1w, 2w, 4w, 6w and 8w). Still, at time points 3d and 4d the lesion volumes were not significantly different between transient and permanent ischemia. From this, It might be concluded that permanent ischemia is causing more severe ischemia whereas early reperfusion salvage penumbra. Previous studies on transient ischemia in rats have shown that reperfusion reduced the extent of initial diffusion lesion when it was performed 95 minutes after the ischemia (Bardutzky et al., 2007) but could broadly diminish the initial diffusion lesions during the early phase of recirculation after 45 to 60 minutes of ischemia (Minematsu et al., 1992, Muller et al., 1995, Neumann-Haefelin et al., 2000, Meng et al., 2004) and could fully revert diffusion lesion within 30 minutes after the onset of ischemia (Li et al., 2000b). In the early time points (2-3 hours after occlusion), Bardutzky et al (Bardutzky et al., 2007) reported approximately 20 % larger lesion volumes in permanent than in 95 minutes transient group. In the present work, at the same time points lesion volumes are approximately 55 % larger in permanent than in 90 minute group. Unfortunately this former study (Bardutzky et al., 2007) scanned the animals only until 3 hours and not further. In good agreement with the work of Bardutzky et al (Bardutzky et al., 2007) who had similar reperfusion time with my work and other works with shorter reperfusion times (Minematsu et al., 1992, Muller et al., 1995, Li et al., 2000b, Neumann-Haefelin et al., 2000, Meng et al., 2004), my study showed evident differences in the evolution of ischemic lesion volume between transient and permanent ischemia.

11 Conclusion

In the present work, significant changes in water ADC and FA were related to ischemic stroke. Moreover, a pathologic condition like brain ischemia causes structural damage to the tissue that give rise to a loss of organization and structure at the cellular level. The changes in water apparent diffusion are thought to be related to changes in brain water content while the changes in anisotropy are linked to changes in tissues microstructure.

In the control animals, FA was higher in the tissues that contain WM than in the GM tissue, which is supporting the idea that this area consists of closely packed and parallel fibers. After permanent and transient MCAO, FA became abnormally low in WM and GM as the loss of the structural integrity appears. However, FA remained significantly higher in WM than in GM throughout the 8 weeks observation period. Relatively higher values in the ischemic WM support the idea that these regions still contain organized axonal structure and do not decrease to the level of isotropic tissues. However, it remains unclear whether these differences are related to the severity of tissue injury. FA normalized in the chronic phase after permanent and transient ischemia, both in WM and GM. Similar normalization has not been reported before and it can be considered as a novel finding.

The study showed that, after permanent and transient MCAO, there are differences in the temporal evolution of FA in different brain tissues. In the acute and subacute phase after permanent MCAO, FA reduced more rapidly and under longer period of time in GM than in WM. After transient MCAO, FA reduced more rapidly in WM than in GM.

While comparing between transient and permanent ischemia, reperfusion accelerated the evolution of ADC, while the other parameters showed only minor difference between these two groups.

From the comparison of lesion volumes, it might be concluded that permanent ischemia is causing more severe ischemia whereas early reperfusion salvage penumbra.

In the future, DTI might play an important role in the evaluation of ischemic brain injury. Both experimental and patient studies have shown that DTI can provide unique information about the temporal and spatial evolution of the stroke. A quantitative characterization of water diffusion in heterogenic brain tissues in the healthy and ischemic brain might offer more detailed information about the tissue damage and help with the further actions after the stroke onset. Finally, diffusion anisotropy measures can be combined with other MR parameters to provide a means of evaluating cerebral ischemia in a time-independent fashion.

12 Bibliography

Ahlhelm, F., Schneider, G., Backens, M., Reith, W. and Hagen, T., 2002. Time course of the apparent diffusion coefficient after cerebral infarction. Eur Radiol. 12, 2322-2329.

Alexander, A. L., Lee, J. E., Lazar, M. and Field, A. S., 2007. Diffusion tensor imaging of the brain. Neurotherapeutics. 4, 316-329.

Anderson, A. W., 2001. Theoretical analysis of the effects of noise on diffusion tensor imaging. Magn Reson Med. 46, 1174-1188.

Arakawa, S., Wright, P. M., Koga, M., Phan, T. G., Reutens, D. C., Lim, I., Gunawan, M. R., Ma, H., Perera, N., Ly, J., Zavala, J., Fitt, G. and Donnan, G. A., 2006. Ischemic thresholds for gray and white matter: a diffusion and perfusion magnetic resonance study. Stroke. 37, 1211-1216.

Armitage, P. A., Bastin, M. E., Marshall, I., Wardlaw, J. M. and Cannon, J., 1998. Diffusion anisotropy measurements in ischaemic stroke of the human brain. Magma. 6, 28-36.

Bardutzky, J., Shen, Q., Henninger, N., Schwab, S., Duong, T. Q. and Fisher, M., 2007. Characterizing tissue fate after transient cerebral ischemia of varying duration using quantitative diffusion and perfusion imaging. Stroke. 38, 1336-1344.

Basser, P. J., Mattiello, J. and LeBihan, D., 1994a. Estimation of the effective self-diffusion tensor from the NMR spin echo. J Magn Reson B. 103, 247-254.

Basser, P. J., Mattiello, J. and LeBihan, D., 1994b. MR diffusion tensor spectroscopy and imaging. Biophys J. 66, 259-267.

Basser, P. J. and Pierpaoli, C., 1996. Microstructural and physiological features of tissues elucidated by quantitative-diffusion-tensor MRI. J Magn Reson B. 111, 209-219.

Bastin, M. E., Armitage, P. A. and Marshall, I., 1998. A theoretical study of the effect of experimental noise on the measurement of anisotropy in diffusion imaging. Magn Reson Imaging. 16, 773-785.

Bastin, M. E., Rana, A. K., Wardlaw, J. M., Armitage, P. A. and Keir, S. L., 2000. A study of the apparent diffusion coefficient of grey and white matter in human ischaemic stroke. Neuroreport. 11, 2867-2874.

Beaulieu, C., 2002. The basis of anisotropic water diffusion in the nervous system - a technical review. NMR Biomed. 15, 435-455.

Benveniste, H., Hedlund, L. W. and Johnson, G. A., 1992. Mechanism of detection of acute cerebral ischemia in rats by diffusion-weighted magnetic resonance microscopy. Stroke. 23, 746-754.

Bloch, F., 1946. Nuclear induction. Phys Rev. 70, 460.

Bristow, M. S., Simon, J. E., Brown, R. A., Eliasziw, M., Hill, M. D., Coutts, S. B., Frayne, R., Demchuk, A. M. and Mitchell, J. R., 2005. MR perfusion and diffusion in acute ischemic stroke: human gray and white matter have different thresholds for infarction. J Cereb Blood Flow Metab. 25, 1280-1287.

Broderick, J., Brott, T., Kothari, R., Miller, R., Khoury, J., Pancioli, A., Gebel, J., Mills, D., Minneci, L. and Shukla, R., 1998. The Greater Cincinnati/Northern Kentucky Stroke Study: preliminary first-ever and total incidence rates of stroke among blacks. Stroke. 29, 415-421.

Brown, M., 2003. MRI Basic Principles and Applications.

Brown, R., 1827. Brownian motion.

Brugieres, P., Thomas, P., Maraval, A., Hosseini, H., Combes, C., Chafiq, A., Ruel, L., Breil, S., Peschanski, M. and Gaston, A., 2004. Water diffusion compartmentation at high b values in ischemic human brain. AJNR Am J Neuroradiol. 25, 692-698.

Bushong, S., 2003. an overview of magnetic resonance imaging. magnetic resonance imaging physical and biological principles. Mosby, Houston.

Carano, R. A., Li, F., Irie, K., Helmer, K. G., Silva, M. D., Fisher, M. and Sotak, C. H., 2000. Multispectral analysis of the temporal evolution of cerebral ischemia in the rat brain. J Magn Reson Imaging. 12, 842-858.

Chan, P. H., 1996. Role of oxidants in ischemic brain damage. Stroke. 27, 1124-1129.

Chepuri, N. B., Yen, Y. F., Burdette, J. H., Li, H., Moody, D. M. and Maldjian, J. A., 2002. Diffusion anisotropy in the corpus callosum. AJNR Am J Neuroradiol. 23, 803-808.

Chien, D., Kwong, K. K., Gress, D. R., Buonanno, F. S., Buxton, R. B. and Rosen, B. R., 1992. MR diffusion imaging of cerebral infarction in humans. AJNR Am J Neuroradiol. 13, 1097-1102; discussion 1103-1095.

Clark, C. A. and Le Bihan, D., 2000. Water diffusion compartmentation and anisotropy at high b values in the human brain. Magn Reson Med. 44, 852-859.

Davis, D., Ulatowski, J., Eleff, S., Izuta, M., Mori, S., Shungu, D. and van Zijl, P. C., 1994. Rapid monitoring of changes in water diffusion coefficients during reversible ischemia in cat and rat brain. Magn Reson Med. 31, 454-460.

Detre, J. A., Leigh, J. S., Williams, D. S. and Koretsky, A. P., 1992. Perfusion imaging. Magn Reson Med. 23, 37-45.

Dietrich, O., Heiland, S., Benner, T. and Sartor, K., 2000. Reducing motion artefacts in diffusion-weighted MRI of the brain: efficacy of navigator echo correction and pulse triggering. Neuroradiology. 42, 85-91.

Doerfler, A., Engelhorn, T., Heiland, S., Benner, T. and Forsting, M., 2002. Perfusion- and diffusion-weighted magnetic resonance imaging for monitoring decompressive craniectomy in animals with experimental hemispheric stroke. J Neurosurg. 96, 933-940.

Durukan, A., Sribian, D. and Tatlisumak, T., 2007a. MRI in drug development for stroke). Department of clinical neurosciences.

Durukan, A., Strbian, D. and Tatlisumak, T., 2007b. Rodent models of ischemic stroke). Department of clinical neuroscience.

Durukan, A. and Tatlisumak, T., 2007. Acute ischemic stroke: overview of major experimental rodent models, pathophysiology, and therapy of focal cerebral ischemia. Pharmacol Biochem Behav. 87, 179-197.

Durukan, A. and Tatlisumak, T., 2009. Animal models of ischemic stroke. In: B.V., E. (Ed.), Handbook of Clinical Neurology, vol.92. M. Fisher.

Emre, U., Rantanen, K. and Tatlisumak, T., 2007. Antithrombotic treatment in the prevention of ischemic stroke. Curr Drug Targets. 8, 817-823.

Englander, S. A., Ulug, A. M., Brem, R., Glickson, J. D. and van Zijl, P. C., 1997. Diffusion imaging of human breast. NMR Biomed. 10, 348-352.

Ewing, J. R., Jiang, Q., Boska, M., Zhang, Z. G., Brown, S. L., Li, G. H., Divine, G. W. and Chopp, M., 1999. T1 and magnetization transfer at 7 Tesla in acute ischemic infarct in the rat. Magn Reson Med. 41, 696-705.

Falcao, A. L., Reutens, D. C., Markus, R., Koga, M., Read, S. J., Tochon-Danguy, H., Sachinidis, J., Howells, D. W. and Donnan, G. A., 2004. The resistance to ischemia of white and gray matter after stroke. Ann Neurol. 56, 695-701.

Fiehler, J., Foth, M., Kucinski, T., Knab, R., von Bezold, M., Weiller, C., Zeumer, H. and Rother, J., 2002. Severe ADC decreases do not predict irreversible tissue damage in humans. Stroke. 33, 79-86.

Fisher, M. and Tatlisumak, T., 2005. Use of animal models has not contributed to development of acute stroke therapies: con. Stroke. 36, 2324-2325.

Ginsberg, M. D., 2003. Adventures in the pathophysiology of brain ischemia: penumbra, gene expression, neuroprotection: the 2002 Thomas Willis Lecture. Stroke. 34, 214-223.

Green, H. A., Pena, A., Price, C. J., Warburton, E. A., Pickard, J. D., Carpenter, T. A. and Gillard, J. H., 2002. Increased anisotropy in acute stroke: a possible explanation. Stroke. 33, 1517-1521.

Gröhn, H., 2003. A study of T1 relaxation: from relaxation mechanism to the magnetic resonance imaging contrast. In: Faculty of natural and environmental sciences), vol. doctoral dissertation. University of Kuopio, Kuopio.

Guilfoyle, D. N., Helpern, J. A. and Lim, K. O., 2003. Diffusion tensor imaging in fixed brain tissue at 7.0 T. NMR Biomed. 16, 77-81.

Hasan, K. M., Gupta, R. K., Santos, R. M., Wolinsky, J. S. and Narayana, P. A., 2005. Diffusion tensor fractional anisotropy of the normal-appearing seven segments of the corpus callosum in healthy adults and relapsing-remitting multiple sclerosis patients. J Magn Reson Imaging. 21, 735-743.

Hasegawa, Y., Fisher, M., Latour, L. L., Dardzinski, B. J. and Sotak, C. H., 1994. MRI diffusion mapping of reversible and irreversible ischemic injury in focal brain ischemia. Neurology. 44, 1484-1490.

Helpern, J., 1992. The effect of cell membrane water permeability on the diffusion coefficient of water. Magn Reson Imaging. 1, 1201.

Helpern, J. A., Dereski, M. O., Knight, R. A., Ordidge, R. J., Chopp, M. and Qing, Z. X., 1993. Histopathological correlations of nuclear magnetic resonance imaging parameters in experimental cerebral ischemia. Magn Reson Imaging. 11, 241-246.

Hennel, F., 1998. Image-based reduction of artifacts in multishot echo-planar imaging. J Magn Reson. 134, 206-213.

Hoehn-Berlage, M., Eis, M., Back, T., Kohno, K. and Yamashita, K., 1995. Changes of relaxation times (T1, T2) and apparent diffusion coefficient after permanent middle cerebral artery occlusion in the rat: temporal evolution, regional extent, and comparison with histology. Magn Reson Med. 34, 824-834.

Ishii, H., Arai, T., Morikawa, S., Inubushi, T., Tooyama, I., Kimura, H. and Mori, K., 1998. Evaluation of focal cerebral ischemia in rats by magnetic resonance imaging and immunohistochemical analyses. J Cereb Blood Flow Metab. 18, 931-934.

Jiang, Q., Chopp, M., Zhang, Z. G., Knight, R. A., Jacobs, M., Windham, J. P., Peck, D., Ewing, J. R. and Welch, K. M., 1997. The temporal evolution of MRI tissue signatures after transient middle cerebral artery occlusion in rat. J Neurol Sci. 145, 15-23.

Jiang, Q., Zhang, Z. G., Chopp, M., Helpern, J. A., Ordidge, R. J., Garcia, J. H., Marchese, B. A., Qing, Z. X. and Knight, R. A., 1993. Temporal evolution and spatial distribution of the diffusion constant of water in rat brain after transient middle cerebral artery occlusion. J Neurol Sci. 120, 123-130.

Jones, D. K., 2004. The effect of gradient sampling schemes on measures derived from diffusion tensor MRI: a Monte Carlo study. Magn Reson Med. 51, 807-815.

Jones, D. K., Horsfield, M. A. and Simmons, A., 1999. Optimal strategies for measuring diffusion in anisotropic systems by magnetic resonance imaging. Magn Reson Med. 42, 515-525.

Kato, H., Kogure, K., Ohtomo, H., Izumiyama, M., Tobita, M., Matsui, S., Yamamoto, E., Kohno, H., Ikebe, Y. and Watanabe, T., 1986. Characterization of experimental ischemic brain edema utilizing proton nuclear magnetic resonance imaging. J Cereb Blood Flow Metab. 6, 212-221.

Kettunen, M. I., Grohn, O. H., Lukkarinen, J. A., Vainio, P., Silvennoinen, M. J. and Kauppinen, R. A., 2000. Interrelations of T(1) and diffusion of water in acute cerebral ischemia of the rat. Magn Reson Med. 44, 833-839.

Kim, S., Pickup, S., Hsu, O. and Poptani, H., 2008. Diffusion tensor MRI in rat models of invasive and well-demarcated brain tumors. NMR Biomed. 21, 208-216.

Knight, R. A., Dereski, M. O., Helpern, J. A., Ordidge, R. J. and Chopp, M., 1994. Magnetic resonance imaging assessment of evolving focal cerebral ischemia. Comparison with histopathology in rats. Stroke. 25, 1252-1261; discussion 1261-1252.

Koizumi, J., Yoshiba, Y., Nakazawa, T. and Ooneda, G., 1986. Experimental studies of ischemic brain edema 1. A new experimental model of cerebral embolism in which reciculation can be introduced in the ischemic area. Jpn J Stroke. 8, 1-8.

Lansberg, M. G., Thijs, V. N., O'Brien, M. W., Ali, J. O., de Crespigny, A. J., Tong, D. C., Moseley, M. E. and Albers, G. W., 2001. Evolution of apparent diffusion coefficient, diffusion-weighted, and T2-weighted signal intensity of acute stroke. AJNR Am J Neuroradiol. 22, 637-644.

Le Bihan, D., 1990. Magnetic resonance imaging of perfusion. Magn Reson Med. 14, 283-292.

Le Bihan, D., 2006. Looking into the architecture of the brain with diffusion MRI. In: Elsevier (Ed.). Proceedings of the. International congress series, pp.

Le Bihan, D., Mangin, J. F., Poupon, C., Clark, C. A., Pappata, S., Molko, N. and Chabriat, H., 2001. Diffusion tensor imaging: concepts and applications. J Magn Reson Imaging. 13, 534-546.

Lee, F. K., Fang, M. R., Antonio, G. E., Yeung, D. K., Chan, E. T., Zhang, L. H., Yew, D. T. and Ahuja, A. T., 2006. Diffusion tensor imaging (DTI) of rodent brains in vivo using a 1.5T clinical MR scanner. J Magn Reson Imaging. 23, 747-751.

Lewis, C. E., Prato, F. S., Drost, D. J. and Nicholson, R. L., 1986. Comparison of respiratory triggering and gating techniques for the removal of respiratory artifacts in MR imaging. Radiology. 160, 803-810.

Li, F., Liu, K. F., Silva, M. D., Omae, T., Sotak, C. H., Fenstermacher, J. D., Fisher, M., Hsu, C. Y. and Lin, W., 2000a. Transient and permanent resolution of ischemic lesions on diffusion-weighted imaging after brief periods of focal ischemia in rats: correlation with histopathology. Stroke. 31, 946-954.

Li, F., Silva, M. D., Sotak, C. H. and Fisher, M., 2000b. Temporal evolution of ischemic injury evaluated with diffusion-, perfusion-, and T2-weighted MRI. Neurology. 54, 689-696.

Lim, K. O. and Helpern, J. A., 2002. Neuropsychiatric applications of DTI - a review. NMR Biomed. 15, 587-593.

Liu, Y., D'Arceuil, H. E., Westmoreland, S., He, J., Duggan, M., Gonzalez, R. G., Pryor, J. and de Crespigny, A. J., 2007. Serial diffusion tensor MRI after transient and permanent cerebral ischemia in nonhuman primates. Stroke. 38, 138-145.

Loubinoux, I., Volk, A., Borredon, J., Guirimand, S., Tiffon, B., Seylaz, J. and Meric, P., 1997. Spreading of vasogenic edema and cytotoxic edema assessed by quantitative diffusion and T2 magnetic resonance imaging. Stroke. 28, 419-426; discussion 426-417.

Lutsep, H. L., Albers, G. W., DeCrespigny, A., Kamat, G. N., Marks, M. P. and Moseley, M. E., 1997. Clinical utility of diffusion-weighted magnetic resonance imaging in the assessment of ischemic stroke. Ann Neurol. 41, 574-580.

Lythgoe, M. F., Thomas, D. L., Calamante, F., Pell, G. S., King, M. D., Busza, A. L., Sotak, C. H., Williams, S. R., Ordidge, R. J. and Gadian, D. G., 2000. Acute changes in MRI diffusion, perfusion, T(1), and T(2) in a rat model of oligemia produced by partial occlusion of the middle cerebral artery. Magn Reson Med. 44, 706-712.

Madi, S., Hasan, K. M. and Narayana, P. A., 2005. Diffusion tensor imaging of in vivo and excised rat spinal cord at 7 T with an icosahedral encoding scheme. Magn Reson Med. 53, 118-125.

Makela, H. I., Kettunen, M. I., Grohn, O. H. and Kauppinen, R. A., 2002. Quantitative T(1rho) and magnetization transfer magnetic resonance imaging of acute cerebral ischemia in the rat. J Cereb Blood Flow Metab. 22, 547-558.

Mamata, H., Jolesz, F. A. and Maier, S. E., 2004. Characterization of central nervous system structures by magnetic resonance diffusion anisotropy. Neurochem Int. 45, 553-560.

Marcoux, F. W., Morawetz, R. B., Crowell, R. M., DeGirolami, U. and Halsey, J. H., Jr., 1982. Differential regional vulnerability in transient focal cerebral ischemia. Stroke. 13, 339-346.

Marks, M. P., de Crespigny, A., Lentz, D., Enzmann, D. R., Albers, G. W. and Moseley, M. E., 1996. Acute and chronic stroke: navigated spin-echo diffusion-weighted MR imaging. Radiology. 199, 403-408.

Marks, M. P., Tong, D. C., Beaulieu, C., Albers, G. W., de Crespigny, A. and Moseley, M. E., 1999. Evaluation of early reperfusion and i.v. tPA therapy using diffusion- and perfusion-weighted MRI. Neurology. 52, 1792-1798.

Masutani, Y., Aoki, S., Abe, O., Hayashi, N. and Otomo, K., 2003. MR diffusion tensor imaging: recent advance and new techniques for diffusion tensor visualization. Eur J Radiol. 46, 53-66.

Meng, X., Fisher, M., Shen, Q., Sotak, C. H. and Duong, T. Q., 2004. Characterizing the diffusion/perfusion mismatch in experimental focal cerebral ischemia. Ann Neurol. 55, 207-212.

Minematsu, K., Li, L., Sotak, C. H., Davis, M. A. and Fisher, M., 1992. Reversible focal ischemic injury demonstrated by diffusion-weighted magnetic resonance imaging in rats. Stroke. 23, 1304-1310; discussion 1310-1301.

Mintorovitch, J., Moseley, M. E., Chileuitt, L., Shimizu, H., Cohen, Y. and Weinstein, P. R., 1991. Comparison of diffusion- and T2-weighted MRI for the early detection of cerebral ischemia and reperfusion in rats. Magn Reson Med. 18, 39-50.

Morvan, D., 1995. In vivo measurement of diffusion and pseudo-diffusion in skeletal muscle at rest and after exercise. Magn Reson Imaging. 13, 193-199.

Moseley, M. E., Cohen, Y., Mintorovitch, J., Chileuitt, L., Shimizu, H., Kucharczyk, J., Wendland, M. F. and Weinstein, P. R., 1990. Early detection of regional cerebral ischemia in cats: comparison of diffusion- and T2-weighted MRI and spectroscopy. Magn Reson Med. 14, 330-346.

Muir, K. W. and Grosset, D. G., 1999. Neuroprotection for acute stroke: making clinical trials work. Stroke. 30, 180-182.

Mukherjee, P., Bahn, M. M., McKinstry, R. C., Shimony, J. S., Cull, T. S., Akbudak, E., Snyder, A. Z. and Conturo, T. E., 2000. Differences between gray matter and white matter water diffusion in stroke: diffusion-tensor MR imaging in 12 patients. Radiology. 215, 211-220.

Mukherjee, P., Berman, J. I., Chung, S. W., Hess, C. P. and Henry, R. G., 2008a. Diffusion tensor MR imaging and fiber tractography: theoretic underpinnings. AJNR Am J Neuroradiol. 29, 632-641.

Mukherjee, P., Chung, S. W., Berman, J. I., Hess, C. P. and Henry, R. G., 2008b. Diffusion tensor MR imaging and fiber tractography: technical considerations. AJNR Am J Neuroradiol. 29, 843-852.

Mulkern, R. V., Gudbjartsson, H., Westin, C. F., Zengingonul, H. P., Gartner, W., Guttmann, C. R., Robertson, R. L., Kyriakos, W., Schwartz, R., Holtzman, D., Jolesz, F. A. and Maier, S. E., 1999. Multi-component apparent diffusion coefficients in human brain. NMR Biomed. 12, 51-62.

Muller, T. B., Haraldseth, O., Jones, R. A., Sebastiani, G., Godtliebsen, F., Lindboe, C. F. and Unsgard, G., 1995. Combined perfusion and diffusion-weighted magnetic resonance imaging in a rat model of reversible middle cerebral artery occlusion. Stroke. 26, 451-457; discussion 457-458.

Munoz Maniega, S., Bastin, M. E., Armitage, P. A., Farrall, A. J., Carpenter, T. K., Hand, P. J., Cvoro, V., Rivers, C. S. and Wardlaw, J. M., 2004. Temporal evolution of water diffusion parameters is different in grey and white matter in human ischaemic stroke. J Neurol Neurosurg Psychiatry. 75, 1714-1718.

Namimoto, T., Yamashita, Y., Sumi, S., Tang, Y. and Takahashi, M., 1997. Focal liver masses: characterization with diffusion-weighted echo-planar MR imaging. Radiology. 204, 739-744.

Naruse, S., Aoki, Y., Takei, R., Horikawa, Y. and Ueda, S., 1991. Effects of atrial natriuretic peptide on ischemic brain edema in rats evaluated by proton magnetic resonance method. Stroke. 22, 61-65.

Neumann-Haefelin, T., Kastrup, A., de Crespigny, A., Yenari, M. A., Ringer, T., Sun, G. H. and Moseley, M. E., 2000. Serial MRI after transient focal cerebral ischemia in rats: dynamics of tissue injury, blood-brain barrier damage, and edema formation. Stroke. 31, 1965-1972; discussion 1972-1963.

Ni, H., Kavcic, V., Zhu, T., Ekholm, S. and Zhong, J., 2006. Effects of number of diffusion gradient directions on derived diffusion tensor imaging indices in human brain. AJNR Am J Neuroradiol. 27, 1776-1781.

Niendorf, T., Dijkhuizen, R. M., Norris, D. G., van Lookeren Campagne, M. and Nicolay, K., 1996. Biexponential diffusion attenuation in various states of brain tissue: implications for diffusion-weighted imaging. Magn Reson Med. 36, 847-857.

Oppenheim, C., Grandin, C., Samson, Y., Smith, A., Duprez, T., Marsault, C. and Cosnard, G., 2001. Is there an apparent diffusion coefficient threshold in predicting tissue viability in hyperacute stroke? Stroke. 32, 2486-2491.

Pantoni, L., Garcia, J. H. and Gutierrez, J. A., 1996. Cerebral white matter is highly vulnerable to ischemia. Stroke. 27, 1641-1646; discussion 1647.

Papadakis, N. G., Murrills, C. D., Hall, L. D., Huang, C. L. and Adrian Carpenter, T., 2000. Minimal gradient encoding for robust estimation of diffusion anisotropy. Magn Reson Imaging. 18, 671-679.

Papadakis, N. G., Xing, D., Houston, G. C., Smith, J. M., Smith, M. I., James, M. F., Parsons, A. A., Huang, C. L., Hall, L. D. and Carpenter, T. A., 1999a. A study of rotationally invariant and symmetric indices of diffusion anisotropy. Magn Reson Imaging. 17, 881-892.

Papadakis, N. G., Xing, D., Huang, C. L., Hall, L. D. and Carpenter, T. A., 1999b. A comparative study of acquisition schemes for diffusion tensor imaging using MRI. J Magn Reson. 137, 67-82.

Pearson, K., 1896. On the form of spurious correlation which may arise when indices are used in the measurement of organs. Proc R Soc London. 60, 489-502.

Pfefferbaum, A. and Sullivan, E. V., 2003. Increased brain white matter diffusivity in normal adult aging: relationship to anisotropy and partial voluming. Magn Reson Med. 49, 953-961.

Pierpaoli, C. and Basser, P. J., 1996. Toward a quantitative assessment of diffusion anisotropy. Magn Reson Med. 36, 893-906.

Pierpaoli, C., Righini, A., Linfante, I., Tao-Cheng, J. H., Alger, J. R. and Di Chiro, G., 1993. Histopathologic correlates of abnormal water diffusion in cerebral ischemia: diffusion-weighted MR imaging and light and electron microscopic study. Radiology. 189, 439-448.

Price, G., Bagary, M. S., Cercignani, M., Altmann, D. R. and Ron, M. A., 2005. The corpus callosum in first episode schizophrenia: a diffusion tensor imaging study. J Neurol Neurosurg Psychiatry. 76, 585-587.

Puddephat, M., 2005. Principles of magnetic resonance imaging (ed. Internet, R.).

Rantanen, K. and Tatlisumak, T., 2004. Secondary prevention of ischemic stroke. Curr Drug Targets. 5, 457-472.

Roberts, T. P. and Schwartz, E. S., 2007. Principles and implementation of diffusion-weighted and diffusion tensor imaging. Pediatr Radiol. 37, 739-748.

Robson, M. D. and Porter, D. A., 2005. Reconstruction as a source of artifact in non-gated single-shot diffusion-weighted EPI. Magn Reson Imaging. 23, 899-905.

Rodriguez-Yanez, M., Castellanos, M., Blanco, M., Mosquera, E. and Castillo, J., 2006. Vascular protection in brain ischemia. Cerebrovasc Dis. 21 Suppl 2, 21-29.

Rothwell, P. M., 2001. The high cost of not funding stroke research: a comparison with heart disease and cancer. Lancet. 357, 1612-1616.

Rudin, M., Baumann, D., Ekatodramis, D., Stirnimann, R., McAllister, K. H. and Sauter, A., 2001. MRI analysis of the changes in apparent water diffusion coefficient, T(2) relaxation time, and cerebral blood flow and volume in the temporal evolution of cerebral infarction following permanent middle cerebral artery occlusion in rats. Exp Neurol. 169, 56-63.

Sakail, K., 2007. Can diffusion tensor imaging detect the degreeof neuronal cell membrane damage in stroke patients? a simulation study. Proceedings of the 5. IASTED International conference, Austria. Biomedical engineering, 14-16, pp.

Schlaug, G., Siewert, B., Benfield, A., Edelman, R. R. and Warach, S., 1997. Time course of the apparent diffusion coefficient (ADC) abnormality in human stroke. Neurology. 49, 113-119.

Schwamm, L. H., Koroshetz, W. J., Sorensen, A. G., Wang, B., Copen, W. A., Budzik, R., Rordorf, G., Buonanno, F. S., Schaefer, P. W. and Gonzalez, R. G., 1998. Time course of lesion development in patients with acute stroke: serial diffusion- and hemodynamic-weighted magnetic resonance imaging. Stroke. 29, 2268-2276.

Skare, S., 2002. Optimisation strategies in diffusion tensor MR imaging. In: MR Center, Department of Clinical Neuroscience). Karolinska Institutet, Stockholm.

Skare, S., Li, T., Nordell, B. and Ingvar, M., 2000. Noise considerations in the determination of diffusion tensor anisotropy. Magn Reson Imaging. 18, 659-669.

Sorensen, A. G., Wu, O., Copen, W. A., Davis, T. L., Gonzalez, R. G., Koroshetz, W. J., Reese, T. G., Rosen, B. R., Wedeen, V. J. and Weisskoff, R. M., 1999. Human acute cerebral ischemia: detection of changes in water diffusion anisotropy by using MR imaging. Radiology. 212, 785-792.

Sotak, C. H., 2002. The role of diffusion tensor imaging in the evaluation of ischemic brain injury - a review. NMR Biomed. 15, 561-569.

Stejskal, E. and Tanner, J., 1965. Spin diffusion measurement: spin echoes in the presence of time dependent field gradient. The Journal of Chemical Physics. 42, 288.

Summers, P., Staempfli, P., Jaermann, T., Kwiecinski, S. and Kollias, S., 2006. A preliminary study of the effects of trigger timing on diffusion tensor imaging of the human spinal cord. AJNR Am J Neuroradiol. 27, 1952-1961.

Tatlisumak, T., 1999. Evaluation of neuroprotective drug effects on experimental focal cerebral ischemia by novel magnetic resonance imaging techniques. In: Department of clinical neurosciences), vol. academic dissertation. Helsinki University, Helsinki.

Tatlisumak, T., Rantanen, K. and Fisher, M., 2007. Stroke prevention: a challenging but rewarding task. Curr Drug Targets. 8, 784-785.

Tatlisumak, T., Takano, K., Carano, R. A., Miller, L. P., Foster, A. C. and Fisher, M., 1998. Delayed treatment with an adenosine kinase inhibitor, GP683, attenuates infarct size in rats with temporary middle cerebral artery occlusion. Stroke. 29, 1952-1958.

Thom, T., Haase, N., Rosamond, W., Howard, V. J., Rumsfeld, J., Manolio, T., Zheng, Z. J., Flegal, K., O'Donnell, C., Kittner, S., Lloyd-Jones, D., Goff, D. C., Jr., Hong, Y., Adams, R., Friday, G., Furie, K., Gorelick, P., Kissela, B., Marler, J., Meigs, J., Roger, V., Sidney, S., Sorlie, P., Steinberger, J., Wasserthiel-Smoller, S., Wilson, M. and Wolf, P., 2006. Heart disease and stroke statistics--2006 update: a report from the American Heart Association Statistics Committee and Stroke Statistics Subcommittee. Circulation. 113, e85-151.

van der Toorn, A., Sykova, E., Dijkhuizen, R. M., Vorisek, I., Vargova, L., Skobisova, E., van Lookeren Campagne, M., Reese, T. and Nicolay, K., 1996. Dynamic changes in water ADC, energy metabolism, extracellular space volume, and tortuosity in neonatal rat brain during global ischemia. Magn Reson Med. 36, 52-60.

van Dorsten, F. A., Olah, L., Schwindt, W., Grune, M., Uhlenkuken, U., Pillekamp, F., Hossmann, K. A. and Hoehn, M., 2002. Dynamic changes of ADC, perfusion, and NMR relaxation parameters in transient focal ischemia of rat brain. Magn Reson Med. 47, 97-104.

van Lookeren Campagne, M., Thomas, G. R., Thibodeaux, H., Palmer, J. T., Williams, S. P., Lowe, D. G. and van Bruggen, N., 1999. Secondary reduction in the apparent diffusion coefficient of water, increase in cerebral blood volume, and delayed neuronal death after middle cerebral artery occlusion and early reperfusion in the rat. J Cereb Blood Flow Metab. 19, 1354-1364.

Warach, S., Chien, D., Li, W., Ronthal, M. and Edelman, R. R., 1992. Fast magnetic resonance diffusion-weighted imaging of acute human stroke. Neurology. 42, 1717-1723.

Warach, S., Gaa, J., Siewert, B., Wielopolski, P. and Edelman, R. R., 1995. Acute human stroke studied by whole brain echo planar diffusion-weighted magnetic resonance imaging. Ann Neurol. 37, 231-241.

Ward, P., Counsell, S., Allsop, J., Cowan, F., Shen, Y., Edwards, D. and Rutherford, M., 2006. Reduced fractional anisotropy on diffusion tensor magnetic resonance imaging after hypoxic-ischemic encephalopathy. Pediatrics. 117, e619-630.

Welch, K. M., Windham, J., Knight, R. A., Nagesh, V., Hugg, J. W., Jacobs, M., Peck, D., Booker, P., Dereski, M. O. and Levine, S. R., 1995. A model to predict the histopathology of human stroke using diffusion and T2-weighted magnetic resonance imaging. Stroke. 26, 1983-1989.

Wick, M., Nagatomo, Y., Prielmeier, F. and Frahm, J., 1995. Alteration of intracellular metabolite diffusion in rat brain in vivo during ischemia and reperfusion. Stroke. 26, 1930-1933; discussion 1934.

Yang, Q., Tress, B. M., Barber, P. A., Desmond, P. M., Darby, D. G., Gerraty, R. P., Li, T. and Davis, S. M., 1999. Serial study of apparent diffusion coefficient and anisotropy in patients with acute stroke. Stroke. 30, 2382-2390.

Zelaya, F., Flood, N., Chalk, J. B., Wang, D., Doddrell, D. M., Strugnell, W., Benson, M., Ostergaard, L., Semple, J. and Eagle, S., 1999. An evaluation of the time dependence of the anisotropy of the water diffusion tensor in acute human ischemia. Magn Reson Imaging. 17, 331-348.

Zhang, K. and Sejnowski, T. J., 2000. A universal scaling law between gray matter and white matter of cerebral cortex. Proc Natl Acad Sci U S A. 97, 5621-5626.

APPENDIX A

Table A1. Absolute mean values of fractional anisotropy and mean diffusivity after permanent MCAO (i.cortex = ischemic cortical regions, c.cortex = contralateral side for ischemic tissue).

PERMANENT ISCHEMIA						
time	*FA*					
	i.cortex	*c.cortex*	*i.subcortex*	*c.subcortex*	*i.corpus callosum*	*c.corpus callosum*
2h	*0.28 (0.07)*	*0.25 (0.03)*	*0.29 (0.05)*	*0.36 (0.09)*	*0.55 (0.06)*	*0.53 (0.09)*
3.5h	*0.23 (0.05)*	*0.22 (0.04)*	*0.25 (0.07)*	*0.33 (0.06)*	*0.49 (0.05)*	*0.52 (0.09)*
1day	*0.17 (0.05)*	*0.25 (0.04)*	*0.15 (0.06)*	*0.35 (0.08)*	*0.36 (0.13)*	*0.49 (0.09)*
2day	*0.10 (0.02)*	*0.23 (0.03)*	*0.14 (0.01)*	*0.37 (0.06)*	*0.30 (0.07)*	*0.45 (0.06)*
3day	*0.08 (0.01)*	*0.23 (0.03)*	*0.17 (0.05)*	*0.36 (0.08)*	*0.36 (0.06)*	*0.45 (0.06)*
4day	*0.07 (0.01)*	*0.22 (0.03)*	*0.17 (0.04)*	*0.36 (0.08)*	*0.38 (0.09)*	*0.44 (0.07)*
1week	*0.10 (0.07)*	*0.23 (0.03)*	*0.23 (0.10)*	*0.41 (0.10)*	*0.41(0.07)*	*0.52 (0.08)*
2week	*0.10 (0.06)*	*0.21 (0.03)*	*0.14 (0.04)*	*0.34 (0.24)*	*0.37 (0.14)*	*0.47 (0.09)*
4week	*0.15 (0.11)*	*0.22 (0.06)*	*0.22 (0.10)*	*0.43 (0.09)*	*0.41 (0.06)*	*0.48 (0.08)*
6week	*0.14 (0.03)*	*0.17 (0.04)*	*0.22 (0.06)*	*0.34 (0.10)*	*0.37 (0.07)*	*0.44 (0.06)*
8week	*0.17 (0.07)*	*0.23 (0.1)*	*0.26 (0.04)*	*0.43 (0.15)*	*0.43 (0.12)*	*0.46 (0.05)*
	ADC x10^{-3}					
	i.cortex	*c.cortex*	*i.subcortex*	*c.subcortex*	*i.corpus callosum*	*c.corpus callosum*
2h	*0.48 (0.15)*	*0.75 (0.06)*	*0.43 (0.10)*	*0.73 (0.06)*	*0.35 (0.09)*	*0.77 (0.14)*
3.5h	*0.42 (0.11)*	*0.70 (0.03)*	*0.34 (0.05)*	*0.67 (0.04)*	*0.47 (0.19)*	*0.71 (0.16)*
1day	*0.47 (0.07)*	*0.70 (0.02)*	*0.46 (0.06)*	*0.69 (0.02)*	*0.40 (0.12)*	*0.67 (0.02)*
2day	*0.50 (0.04)*	*0.69 (0.02)*	*0.50 (0.07)*	*0.69 (0.02)*	*0.36 (0.13)*	*0.67 (0.02)*
3day	*0.56 (0.05)*	*0.70 (0.02)*	*0.47 (0.07)*	*0.68 (0.01)*	*0.39 (0.25)*	*0.69 (0.15)*
4day	*0.58(0.06)*	*0.70 (0.02)*	*0.38 (0.05)*	*0.67 (0.02)*	*0.43 (0.27)*	*0.64 (0.04)*
1week	*0.55 (0.07)*	*0.69 (0.05)*	*0.36 (0.09)*	*0.66 (0.05)*	*0.33 (0.22)*	*0.65 (0.14)*
2week	*0.70 (0.20)*	*0.72 (0.03)*	*0.52 (0.16)*	*0.68 (0.05)*	*0.79 (0.23)*	*0.79 (0.12)*
4week	*0.88 (0.22)*	*0.75 (0.06)*	*0.68 (0.12)*	*0.69 (0.05)*	*0.86 (0.21)*	*0.82 (0.15)*
6week	*0.99 (0.22)*	*0.75 (0.05)*	*0.79 (0.09)*	*0.73 (0.07)*	*0.85 (0.27)*	*0.68 (0.08)*
8week	*1.07 (0.32)*	*0.81 (0.06)*	*0.97 (0.21)*	*0.71 (0.08)*	*0.96 (0.24)*	*0.86 (0.15)*

Table A2. Absolute mean values of T2 and T1 after permanent MCAO (i.cortex = ischemic cortical regions, c.cortex = contralateral side for ischemic tissue).

PERMANENT ISCHEMIA						
time	***T2***					
	i.cortex	***c.cortex***	***i.subcortex***	***c.subcortex***	***i.corpus callosum***	***c.corpus callosum***
2h	***60.8 (3.7)***	***55.7 (1.2)***	***61.1 (3.1)***	***54.8 (3.0)***	***50.8 (4.8)***	***55.2 (14.8)***
3.5h	***62.8 (5.4)***	***55.1 (1.5)***	***62.9 (2.1)***	***54.5 (2.2)***	***55.3 (6.3)***	***52.6 (6.9)***
1day	***94.7 (15.0)***	***56.5 (1.2)***	***91.5 (7.7)***	***56.3 (1.9)***	***60.9 (13.4)***	***51.9 3.1()***
2day	***103.1 (21.3)***	***57.2 (1.0)***	***95.0 (8.2)***	***57.7 (3.2)***	***85.0 (25.6)***	***52.7 (4.2)***
3day	***92.6 (12.2)***	***57.1 (1.9)***	***90.6 (7.7)***	***56.8 (1.9)***	***87.8 (31.0)***	***58.3 (18.9)***
4day	***87.8 (12.7)***	***57.0 (2.0)***	***88.7 (6.9)***	***56.0 (1.8)***	***101.5 (36.2)***	***52.2 (2.2)***
1week	***79.1 (9.4)***	***56.3 (3.1)***	***95.1 (13.2)***	***54.1 (3.1)***	***93.8 (42.7)***	***52.2 (5.5)***
2week	***88.3 (9.7)***	***56.0 (1.0)***	***113.7 (27.1)***	***54.5 (1.6)***	***69.6 (36.1)***	***53.2 (7.4)***
4week	***106.4 (36.2)***	***55.7 (1.8)***	***103.5 (45.6)***	***53.6 (1.5)***	***49.9 (2.9)***	***51.3 (3.5)***
6week	***101.3 (11.5)***	***54.3 (1.8)***	***102.3 (68.6)***	***52.5 (2.4)***	***50.4 (2.8)***	***51.7 (3.7)***
8week	***98.4 (25.6)***	***56.3 (4.3)***	***83.4 (49.1)***	***52.6 (3.0)***	***52.2 (3.2)***	***49.3 (2.1)***
	T1					
	i.cortex	***c.cortex***	***i.subcortex***	***c.subcortex***	***i.corpus callosum***	***c.corpus callosum***
2h	***1725 (136)***	***1513 (85)***	***1637 (146)***	***1406 (100)***	***1394 (197)***	***1403 (224)***
3.5h	***1721 (202)***	***1546 (100)***	***1622 (127)***	***1414 (99)***	***1370 (116)***	***1347 (137)***
1day	***1829 (357)***	***1573 (100)***	***1785 (187)***	***1456 (98)***	***1652 (209)***	***1426 (268)***
2day	***1822 (280)***	***1646 (306)***	***1698 (167)***	***1425 (119)***	***1758 (209)***	***1453 (161)***
3day	***1751 (165)***	***1542 (64)***	***1645 (150)***	***1445 (100)***	***1607 (337)***	***1347 (235)***
4day	***1700 (111)***	***1516 (52)***	***1591 (158)***	***1386 (39)***	***1734 (408)***	***1312 (156)***
1week	***1673 (140)***	***1503 (78)***	***1747 (200)***	***1332 (91)***	***1707 (361)***	***1316 (159)***
2week	***1919 (200)***	***1475 (43)***	***1964 (161)***	***1305 (87)***	***1639 (370)***	***1540 (483)***
4week	***2324 (543)***	***1525 (64)***	***2119 (144)***	***1291 (91)***	***1354 (123)***	***1317 (194)***
6week	***2380 (459)***	***1499 (76)***	***1870 (300)***	***1265 (130)***	***1647 (476)***	***1232 (260)***
8week	***2363 (505)***	***1573 (224)***	***2083 (317)***	***1346 (179)***	***1401 (105)***	***1244 (138)***

APPENDIX B

Table B1. Absolute mean values of fractional anisotropy and mean diffusivity after transient MCAO (i.cortex = ischemic cortical regions, c.cortex = contralateral side for ischemic tissue).

TRANSIENT ISCHEMIA						
time	***FA***					
	i.cortex	***c.cortex***	***i.subcortex***	***c.subcortex***	***i.corpus callosum***	***c.corpus callosum***
2h	***0.19 (0.07)***	***0.20 (0.02)***	***0.21 (0.08)***	***0.29 (0.06)***	***0.38 (0.11)***	***0.45 (0.11)***
3.5h	***0.19 (0.04)***	***0.18 (0.04)***	***0.20 (0.07)***	***0.26 (0.06)***	***0.40 (0.07)***	***0.45 (0.08)***
1day	***0.14 (0.04)***	***0.20 (0.04)***	***0.14 (0.04)***	***0.32 (0.04)***	***0.30 (0.10)***	***0.41 (0.06)***
2day	***0.14 (0.06)***	***0.21 (0.03)***	***0.14 (0.03)***	***0.30 (0.06)***	***0.26 (0.09)***	***0.44 (0.05)***
3day	***0.11 (0.05)***	***0.20 (0.06)***	***0.14 (0.05)***	***0.31 (0.08)***	***0.22 (0.09)***	***0.41 (0.05)***
4day	***0.19 (0.04)***	***0.11 (0.04)***	***0.15 (0.05)***	***0.29 (0.03)***	***0.25 (0.11)***	***0.49 (0.08)***
1week	***0.19 (0.04)***	***0.12 (0.07)***	***0.21 (0.08)***	***0.30 (0.06)***	***0.29 (0.08)***	***0.43 (0.06)***
2week	***0.11 (0.03)***	***0.15 (0.03)***	***0.17 (0.03)***	***0.30 (0.05)***	***0.36 (0.05)***	***0.40 (0.05)***
4week	***0.10 (0.01)***	***0.13 (0.02)***	***0.17 (0.06)***	***0.20 (0.02)***	***0.36 (0.5)***	***0.44 (0.05)***
6week	***0.10 (0.02)***	***0.15 (0.03)***	***0.18 (0.09)***	***0.23 (0.05)***	***0.42 (0.06)***	***0.42 (0.05)***
8week	***0.10 (0.03)***	***0.16 (0.04)***	***0.22 (0.06)***	***0.24 (0.07)***	***0.42 (0.04)***	***0.44 (0.06)***
	ADC x10^{-3}					
	i.cortex	***c.cortex***	***i.subcortex***	***c.subcortex***	***i.corpus callosum***	***c.corpus callosum***
2h	***0.44 (0.18)***	***0.73 (0.07)***	***0.45 (0.09)***	***0.69 (0.06)***	***0.53 (0.21)***	***0.69 (0.04)***
3.5h	***0.48 (0.19)***	***0.76 (0.09)***	***0.43 (0.08)***	***0.71 (0.08)***	***0.48 (0.16)***	***0.70 (0.07)***
1day	***0.54 (0.12)***	***0.73 (0.03)***	***0.50 (0.06)***	***0.69 (0.03)***	***0.58 (0.14)***	***0.69 (0.03)***
2day	***0.59 (0.11)***	***0.74 (0.02)***	***0.53 (0.04)***	***0.70 (0.03)***	***0.82 (0.18)***	***0.69 (0.03)***
3day	***0.63 (0.10)***	***0.73 (0.07)***	***0.57 (0.03)***	***0.71 (0.06)***	***0.90 (0.11)***	***0.67 (0.07)***
4day	***0.63 (0.12)***	***0.74 (0.07)***	***0.63 (0.11)***	***0.70 (0.07)***	***0.82 (0.11)***	***0.68 (0.08)***
1week	***0.72 (0.08)***	***0.75 (0.05)***	***0.62 (0.05)***	***0.70 (0.05)***	***0.78 (0.14)***	***0.70 (0.06)***
2week	***1.00 (0.40)***	***0.78 (0.04)***	***0.76 (0.17)***	***0.72 (0.04)***	***0.85 (0.09)***	***0.74 (0.04)***
4week	***1.27 (0.30)***	***0.78 (0.05)***	***1.01 (0.29)***	***0.72 (0.04)***	***0.91 (0.09)***	***0.72 (0.07)***
6week	***1.29 (0.51)***	***0.79 (0.03)***	***1.15 (0.16)***	***0.72 (0.03)***	***0.91 (0.23)***	***0.72 (0.03)***
8week	***1.29 (0.45)***	***0.77 (0.06)***	***0.95 (0.22)***	***0.67 (0.03)***	***0.87 (0.15)***	***0.72 (0.03)***

Table B2. Absolute mean values of T2 and T1 after transient MCAO (i.cortex = ischemic cortical regions, c.cortex = contralateral side for ischemic tissue).

TRANSIENT ISCHEMIA						
time	***T2***					
	i.cortex	***c.cortex***	***i.subcortex***	***c.subcortex***	***i.corpus callosum***	***c.corpus callosum***
2h	***71.8 (3.6)***	***59.0 (5.5)***	***66.2 (3.8)***	***55.8 (1.6)***	***60.9 (6.8)***	***53.5 (2.8)***
3.5h	***78.8 (10.5)***	***58.9 (5.5)***	***71.7 (14.1)***	***55.5 (2.4)***	***63.4 (7.0)***	***53.1 (3.1)***
1day	***107.8 (25.6)***	***59.2 (5.4)***	***101.8 (14.1)***	***56.4 (2.3)***	***84.7 (26.4)***	***54.1 (2.8)***
2day	***105.7 (17.8)***	***57.4 (3.7)***	***101.8 (12.5)***	***57.4 (1.4)***	***89.5 (21.4)***	***53.4 (1.8)***
3day	***98.4 (5.3)***	***58.9 (4.5)***	***92.3 (5.8)***	***57.3 (1.9)***	***92.7 (13.0)***	***55.3 (1.6)***
4day	***87.8 (9.8)***	***58.6 (4.3)***	***83.9 (11.3)***	***55.6 (1.9)***	***78.6 (18.2)***	***53.2 (3.7)***
1week	***85.7 (11.9)***	***58.3 (5.0)***	***71.6 (5.6)***	***55.7 (1.7)***	***74.0 (17.2)***	***54.1 (2.5)***
2week	***102.8 (42.1)***	***58.0 (1.4)***	***73.1 (5.3)***	***55.6 (2.6)***	***55.3 (3.3)***	***53.0 (3.0)***
4week	***164.8 (50.0)***	***60.0 (3.4)***	***92.9 (28.3)***	***56.3 (2.6)***	***53.7 (3.3)***	***51.1 (3.8)***
6week	***204.7 (129.8)***	***62.0 (5.1)***	***88.6 (32)***	***56.4 (0.64)***	***53.0 (1.9)***	***52.1 (1.6)***
8week	***152.8 (71.7)***	***63.2 (4.7)***	***72.1 (12.1)***	***56.7 (1.8)***	***54.6 (6.2)***	***54.0 (6.6)***
	T1					
	i.cortex	***c.cortex***	***i.subcortex***	***c.subcortex***	***i.corpus callosum***	***c.corpus callosum***
2h	***1697 (60)***	***1574 (117)***	***1609 (115)***	***1457 (104)***	***1470 (78)***	***1371 (116)***
3.5h	***1805 (122)***	***1587 (106)***	***1678 (121)***	***1475 (105)***	***1522 (111)***	***1389 (98)***
1day	***2069 (227)***	***1581 (118)***	***1998 (137)***	***1449 (93)***	***1688 (267)***	***1397 (124)***
2day	***1997 (180)***	***1573 (84)***	***1894 (125)***	***1459 (49)***	***1777 (246)***	***1375 (102)***
3day	***1882 (97)***	***1550 (92)***	***1827 (97)***	***1472 (48)***	***1895 (265)***	***1347 (98)***
4day	***1889 (134)***	***1606 (101)***	***1787 (129)***	***1434 (66)***	***1752 (276)***	***1336 (174)***
1week	***1898 (147)***	***1549 (119)***	***1619 (114)***	***1416 (100)***	***1649 (239)***	***1368 (134)***
2week	***2112 (382)***	***1605 (82)***	***1790 (69)***	***1451 (82)***	***1395 (142)***	***1251 (113)***
4week	***2849 (460)***	***1641 (127)***	***2081 (395)***	***1501 (81)***	***1466 (245)***	***1357 (149)***
6week	***2999 (756)***	***1751 (144)***	***2235 (352)***	***1490 (63)***	***1571 (344)***	***1368 (162)***
8week	***2892 (785)***	***1737 (72)***	***1862 (381)***	***1489 (58)***	***1527 (316)***	***1404 (189)***